AD-A096 098 NAVAL OCEAN SYSTEMS CENTER SAN DIEGO CA F/G 20/14
LF DAYTIME EARTH IONOSPHERE WAVEGUIDE CALCULATIONS.(U)
JAN 81 R A PAPPERT
UNCLASSIFIED NOSC/TR-647 DNA-MIPR-81-504

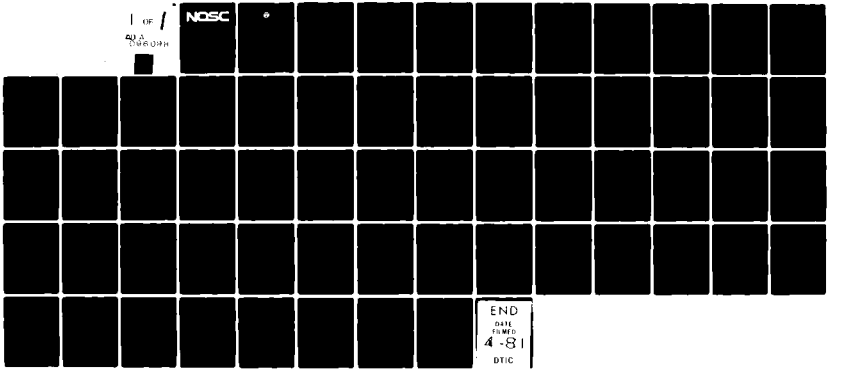

(12)

NOSC

NOSC TR 647

LEVEL II

NOSC TR 647

Technical Report 647

LF DAYTIME EARTH IONOSPHERE WAVEGUIDE CALCULATIONS

AD A096098

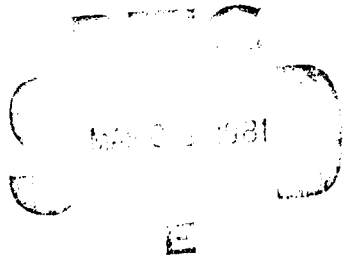

RA Pappert

January 1981

Prepared for
Defense Nuclear Agency
Subproject S99QAXHB,
Work Unit 00001

NAVAL OCEAN SYSTEMS CENTER
SAN DIEGO, CALIFORNIA 92152

NAVAL OCEAN SYSTEMS CENTER, SAN DIEGO, CA 92152

AN ACTIVITY OF THE NAVAL MATERIAL COMMAND

SL GUILLE, CAPT, USN
Commander

HL BLOOD
Technical Director

ADMINISTRATIVE INFORMATION

This work, sponsored by the Defense Nuclear Agency under Program Element 62715H, Subproject S99QAXHB, and work unit 00001 (NOSC 532-MP20), was performed during the period 1 June 1980 through 1 January 1981.

The author is very grateful to LR Shockey for programming and plotting assistance.

Released by
JH Richter, Head
EM Propagation Division

Under authority of
JD Hightower, Head
Environmental Sciences Department

METRIC CONVERSION

To convert from	To	Multiply by
gauss	teslas (T)	10^{-4}
degrees (angle)	radians (rad)	1.75×10^{-2}

UNCLASSIFIED

SECURITY CLASSIFICATION OF THIS PAGE (When Data Entered)

REPORT DOCUMENTATION PAGE	READ INSTRUCTIONS BEFORE COMPLETING FORM
1. REPORT NUMBER NOSC Technical Report 647 (TR 647)	2. GOVT ACCESSION NO. AD-A096 098	3. RECIPIENT'S CATALOG NUMBER
4. TITLE (and Subtitle) LF DAYTIME EARTH IONOSPHERE WAVEGUIDE CALCULATIONS	5. TYPE OF REPORT & PERIOD COVERED Interim 1 Jun 80–Jan 81
	6. PERFORMING ORG. REPORT NUMBER
7. AUTHOR(s) R.A. Pappert	8. CONTRACT OR GRANT NUMBER(s) DNA-MIPR-81-504
9. PERFORMING ORGANIZATION NAME AND ADDRESS Naval Ocean Systems Center San Diego, CA 92152	10. PROGRAM ELEMENT, PROJECT, TASK AREA & WORK UNIT NUMBERS 62715H S99QAXHB, 00001 (NOSC 532-MP20)
11. CONTROLLING OFFICE NAME AND ADDRESS Defense Nuclear Agency Washington, DC 20350	12. REPORT DATE Jan 81 13. NUMBER OF PAGES 58
14. MONITORING AGENCY NAME & ADDRESS (if different from Controlling Office)	15. SECURITY CLASS. (of this report) Unclassified 15a. DECLASSIFICATION DOWNGRADING SCHEDULE

16. DISTRIBUTION STATEMENT (of this Report)

Approved for public release; distribution unlimited

17. DISTRIBUTION STATEMENT (of the abstract entered in Block 20, if different from Report)

18. SUPPLEMENTARY NOTES

19. KEY WORDS (Continue on reverse side if necessary and identify by block number)

EM propagation
Low frequency (lf)
Earth ionosphere waveguide

20. ABSTRACT (Continue on reverse side if necessary and identify by block number)

This report presents results based on waveguide formalism of a numerical study of daytime propagation in the low frequency (lf) band (30–300 kHz). Results are presented for the vertical electric field produced by vertical electric dipole excitation. Ground-to-ground, air-to-air, ground-to-air, and air-to-ground configurations are considered. The results point out the severity of multipath fading, even under daytime conditions, for the upper lf band. The results should be particularly useful as a basis against which to compare the results of alternative methods. Minor waveguide modifications which allow for treatment of whispering gallery type modes are discussed. For the prototype ionosphere considered in this sutdy there is no "low loss" mode of propagation of the latter type.

DD FORM 1 JAN 73 1473 EDITION OF 1 NOV 65 IS OBSOLETE
S/N 0102-LF-014-6601

UNCLASSIFIED

SECURITY CLASSIFICATION OF THIS PAGE (When Data Entered)

OBJECTIVE

Examine the feasibility of using waveguide methods throughout the LF band (30-300 kHz) for a prototype daytime ionosphere.

RESULTS

1. On the basis of the present study it appears feasible to perform waveguide case studies throughout the LF band for daytime as well as for PCA or artificially depressed ionospheres.

2. Production runs would, however, depend upon quicker ionospheric reflection methods as well as improved mode search capability.

3. Extension to nighttime ionospheres as well as into the MF band (300-3000 kHz) could require development of alternative methods.

RECOMMENDATIONS

1. Improve mode search methods and simplify ionospheric full wave reflection calculations for application of waveguide methods to the upper LF band and above.

2. Investigate the utility of "hybrid" methods whereby fields are calculated by combining waveguide and wave hop methods.

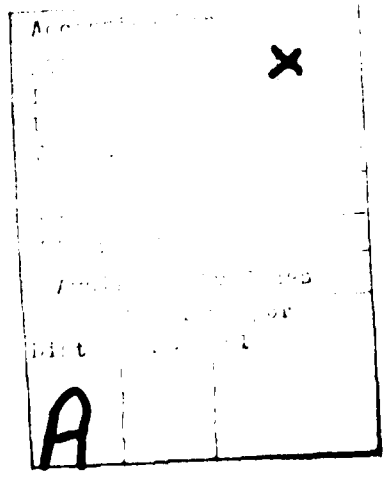

CONTENTS

ILLUSTRATIONS

ILLUSTRATIONS (Continued)

TABLES

1 INTRODUCTION

The prediction of the effect of the propagation medium on radio communication systems operating in the upper LF (>100 kHz) and MF (300 kHz - 3 MHz) bands has lagged considerably behind predictive capability for the adjacent VLF (3-30 kHz) and HF (3 MHz-30 MHz) bands. This has been partly due to the complexity of the propagation theory appropriate to the LF and MF bands and partly due to a lack of operational requirement. With regard to the latter, there has been speculation that whispering gallery type modes (i.e. an rf wave launched at shallow angles along the lower boundary of the D-layer of the ionosphere) should be characterized by low propagation losses and that the use of these modes could provide long range air-to-air communication links.[1,2] It is that speculation which has motivated the present study. Although on the basis of the work reported in references 1 and 2 the MF band appeared to be the preferable of the two bands, we have in this study restricted the effort to the rather modest goal of waveguide application throughout the LF band for a prototype daytime ionosphere.

Wave hop[3-7] techniques have been classically used in the LF band, principally for ground-to-ground transmission. Some wave hop calculations for elevated antennas have only recently been reported[8] and we will make comparisons with some of those results. The present study extends considerably the existing catalogue of daytime-LF numerical results. It also demonstrates the feasibility of using waveguide concepts for case studies of propagation under daytime conditions and, probably, for studies of LF propagation in PCA and nuclear-disturbed environments. Use for production applications, and possibly for nighttime conditions, would probably require improvement of the mode search techniques as well as the replacement of full-wave ionospheric reflection calculations by either phase integral or a combination of phase

integral and full-wave methods. One of the attractive possibilities in future studies for speedier calculations in the LF band and possibly extension into the MF band would be the so called "hybrid" methods[9-12] whereby fields are calculated by combining waveguide and hop methods.

In the following section minor modifications of the programs documented in references 13 and 14, which allow for treatment of whispering gallery type modes, are discussed. In section 3 the prototype ionosphere is documented. To check results presented in reference 8, a limited number of calculations have also been generated for Deeks'[15] summertime profile. Data for that profile are also documented in section 3. In section 4 results are presented and following that the conclusions and recommendations are summarized.

2 SUMMARY OF EQUATIONS

The waveguide program documented in reference 13 and the excitation and height gain formulas documented in reference 14 serve as the basis for the present study. Table 1 below lists the real (θ_r) and imaginary (θ_i) part of the eigenangle and the magnitude of an excitation factor, $|\lambda|$, for ground-based excitation of the first mode (mode numbering begins with the eigenangle having the largest real part) as a function of frequency. More complete documentation and description of mode data are presented in section 4. For the present it is only necessary to appreciate the fact that the excitation factor gives a measure of how well a ground-based antenna would excite the first order mode and that the first order mode becomes more and more earth detached (or equivalently more of a whispering gallery type mode) as the frequency increases.

Table 1 Eigenangles and Excitation Factors

Freq (kHz)	θ_r (°)	θ_i (°)	$\|\lambda\|$
100	86.098	-0.335	3.2×10^{-9}
150	86.732	-0.378	1.6×10^{-12}
200	87.141	-0.417	6.3×10^{-17}
250	87.438	-0.455	5.1×10^{-21}
300	87.670	-0.493	2.7×10^{-16}

The tabulations in Table 1 are consistent with the program documented in reference 13 and are for the prototype daytime ionosphere described in the following section. The significant feature of Table 1 is that the excitation factor does not monotonically decrease with frequency as it should (i.e. the more earth-detached the mode the poorer its excitation by a ground-based source). The reason for the incorrect behavior is that the linear combination of modified Hankel functions of order one third used to represent the height gain at the ground is in fact incorrect at the ground for modes which are

highly earth detached. To correct for this deficiency we have opted to throw away earth effects altogether when the condition

$$\text{Re}\left[2i\,(k/\alpha)(C_H^2 - \alpha H)^{3/2}/3\right] > 12.4 \tag{1}$$

is met. The quantity within the brackets relates to the degree of evanescence of the height gain at the ground, and the value 12.4 on the right-hand side of (1) has been selected on the basis of trial and error. It requires the degree of evanescence at the ground to be of the order of several times 10^{-6} (i.e. the magnitude of the modal height gain is down by more than 100 dB from its value near the base of the D layer). When condition (1) is satisfied, the plane wave reflection coefficients $_{\parallel}\bar{R}_{\parallel d}$ and $_{\perp}\bar{R}_{\perp d}$ referenced to level d become

$$_{\parallel}\bar{R}_{\parallel d} = \frac{C_H h(q_d) + F(q_d)}{C_H h(q_d) - F(q_d)} \tag{2}$$

$$_{\perp}\bar{R}_{\perp d} = \frac{C_H h(q_d) + i(\alpha/k)^{1/3}\, h'(q_d)}{C_H h(q_d) - i(\alpha/k)^{1/3}\, h'(q_d)}\ , \tag{3}$$

where the subscripts $\parallel$ denote TM polarization for both the downgoing and upgoing wave and the subscripts $\perp$ denote TE polarization for the downgoing and upgoing wave. Also,

$C_H = \cos(\theta)$

θ = eigenangle referenced to level H

$q_z = (k/\alpha)^{2/3}\left[C_H^2 + \alpha(z-H)\right]$

k = wave number

$\alpha = 2/a$

a = earth's radius

d = altitude at which modal equation is evaluated

H = altitude at which modified refractive index is taken to be unity

$h = h_2 - \exp(i4\pi/3)h_1$

h_2, h_1 = modified Hankel functions of order one third

$i = \sqrt{-1}$

$F(q_d) = i\left[0.5(\alpha/k)h(q_d) + (\alpha/k)^{1/3}\, h'(q_d)\right]/n^2(d)$

$n(d)$ = modified refractive index at height d

$\bar{R}_d$ = plane wave reflection coefficient looking down from level d

The subscript H on the Cs indicate that the eigenangle is referenced to height H where the modified refractive index is unity. Also, the prime on h in equation (3) and in the expression for F denotes a derivative with respect to the argument.

It should be mentioned that the waveguide program of reference 13 does in fact find the correct eigenangles for the cases studied in this report even though the starting conditions at the ground are incorrect for calculation of the $\bar{R}_d$ values. The reason for this is that the admixture of incorrect solutions decays with altitude, and for whispering gallery type calculations the mode equation is evaluated at the base of the D layer (typically at altitudes >50 km) so that the process is in a sense self correcting. Nevertheless, it seemed to us better to use equations (2) and (3) under the appropriate conditions rather than risk the possibility of error when parameter sets change.

We now turn to a discussion of the mode sum calculation used in this study. Apart from the minor replacements to be discussed, the formulas for mode summing are given in reference 14. The minor replacements just referred to concern height gain replacements which must be made when the test given in (1) is passed. Specifically, equations (2) and (3) of reference 14 are to be

replaced by

$$f_{\parallel}(z) = \exp[(z-a)/2]h(q_z) \quad \text{(replacement for eq. (2) of ref. 14 when (1) passes).} \tag{4}$$

$$f_{\perp}(z) = h(q_z) \quad \text{(replacement for eq. (3) of ref. 14 when (1) passes).} \tag{5}$$

Consistent with reference 14, the mode sum evaluation for the vertical electric field, E_z, for a vertical dipole source is

$$E_z(\text{volts/m per kW}) = 6.807 \times 10^{-4} \sqrt{\frac{\nu}{\sin(x/a)}}$$

$$\cdot \sum_p G_p f_{\parallel}(z_R) f_{\parallel}(z_T) \exp(-ik(S_{po} - 1)x), \tag{6}$$

where p is the mode index and

ν = frequency in kHz

x = transmitter receiver distance

$G_p = S_p^{5/2} (1+{}_{\parallel}R_{\parallel d})^2 (1-{}_{\perp}\bar{R}_{\perp d}\, {}_{\perp}R_{\perp d})/\left|{}_{\parallel}\bar{R}_{\parallel d} \frac{\partial F}{\partial \theta} f_{\parallel}^2(d)\right|$

$\frac{\partial F}{\partial \theta}$ = derivative of the modal equation evaluated at $\theta = \theta_p$

S_p = sine of eigenangle referenced to height H

S_{po} = sine of eigenangle referenced to ground level (i.e. z = 0)

As stated above, the formulas of reference 14 are to be used for $f_{\parallel}$ and $f_{\perp}$ if test (1) is not passed whereas equations (4) and (5) are to be used if the test is passed. The subscripts R and T on z in equation (6) signify the receiver and transmitter altitudes respectively.

Finally, the height gain replacements (4) and (5) are also incorporated into the waveguide program of reference 13 when test 1 is passed. This inclusion eliminates the excitation factor dilemma discussed earlier in this section.

3 DESCRIPTION OF IONOSPHERIC PROFILES

The majority of calculations were made by using the lower extremities of the GE-TEMPO ambient day profile.[16] Only electrons have been included in the profile, and their height dependence as well as that of the collision frequency are shown in Table 2. The variation between tabulated points is assumed to be exponential. Though the D-region electron density model has been taken from Knapp, it has no special significance and is used in this study simply to demonstrate the feasibility of carrying out waveguide calculations throughout the LF band for a prototype daytime ionosphere. The profile has been truncated at 80 km since most of the LF reflections occur below that level.

A limited number of calculations, made to check our results with those based on a wave hop program, have been performed for the Deeks' summertime day profile shown in Table 3.

The GE-TEMPO and Deeks' profiles are schematized in Figure 1. Above about 64 km the GE-TEMPO number densities exceed those of the Deeks' profile by factors varying between about 2 and 4. This tends to make the results for the GE-TEMPO profile more lossy than the Deeks' profile, so that the mean decay of the signal for the GE-TEMPO profile will be somewhat greater. In a comparison with data this difference would be quite significant; but for the principal purpose of this study—namely the demonstration of the feasibility of carrying out waveguide calculations throughout the LF band for daytime (and presumably depressed) conditions—the difference is of no significant consequence.

4 RESULTS

This section contains a variety of range and height gain curves for propagation over sea. The bulk of the curves are for the GE-TEMPO profile and are for frequencies of 100, 150, 200, 250 and 300 kHz. Included are rather complete mode set tabulations. The number of modes range from a dozen at 100 kHz to 28 at 300 kHz. The MODESRCH[17] algorithm was used to find the mode set for the 100 and 150 kHz cases. Above 150 kHz however, numerical problems with MODESRCH were encountered and the modes were generated by using the trace routine described by Ferguson.[18] Although the latter does not infallibly locate all significant modes, missing modes can usually be spotted by scrutinizing the mode set (particularly as regards mode excitation and polarizations as well as mode structure at the previous frequency). They can then be located by inputs of a variety of prudently selected trial starting eigenangles. Obviously this procedure could be made much more cost effective by modifications to MODESRCH which would allow that method to be used at higher frequencies. Very likely, too, the trace routine of Ferguson could be improved. These are areas of improvement recommended for future work.

Figures 2 through 4 show comparisons between range calculations of Campbell and Jones[8], who used a wave hop analysis, and the waveguide calculations of this study. The calculations are for the Deeks' summertime day profile at 150 kHz. Figure 2 applies to ground-to-ground propagation, Figure 3 is for ground transmission to a receiver at 5 km, and Figure 4 is for ground transmission to a receiver at 9 km. The waveguide curves have been generated for a geomagnetic field of 0.4508 Gauss, a dip angle of 65.82° and an azimuth of 0°. Since Campbell and Jones specified only the azimuth, latitude and longitude for which their calculations applied, the preceding geomagnetic conditions may be at slight variance with theirs. Also, the digital input for

the electron density and collision frequency may vary slightly from their input. Differences of this sort could be responsible for the slight discrepancies between the waveguide and wave hop calculations. In view of the difference in methods, the agreement between the two sets of calculations seems to us quite remarkable. To our knowledge Figures 3 and 4 show for the first time comparisons between waveguide calculations and the wave hop method for elevated antennas.

Table 4 contains the set of mode data upon which the waveguide calculations in Figures 2 through 4 are based. The first column gives the mode numbering beginning with the eigenangle which has the largest real part (i.e. the most grazing or earth detached mode). Eighteen modes have been included in the set. The second and third columns give the real and imaginary parts of the modal eigenangle expressed in degrees and referenced to height H. For the calculations shown in Table 4, H was set to 56 km. The fourth column gives the modal attenuation rates, which range between about 8.7 dB/Mm and 36 dB/Mm. It is interesting to note that the modal attenuation rate for the ninth mode is only about 0.8 dB/Mm greater than the attenuation rate for the first mode (i.e. the most pronounced whispering gallery mode). There are in this instance about 10 modes with attenuation rates comparable to the least attenuated mode but no modes with exceptionally low attenuation rates as one might anticipate for modes characterized by very grazing incidence angles. This is because daytime ionospheres are not particularly abrupt and there is generally an appreciable ionospheric absorption at altitudes below the height where the bulk of the reflection occurs. We would anticipate this modal feature to be much the same for PCA or artificially depressed ionospheres but to be quite different for propagation beneath an ambient nighttime ionosphere. The fifth column gives the ratio of the modal phase velocity to the speed of light in

vacuum. The sixth and seventh columns give the magnitude and phase (in radians) of an excitation factor defined as

$$|\lambda| e^{i\phi} = \frac{s_p^{5/2} \, (1+{}_{\parallel}\bar{R}_{\parallel d})^2 \, (1-{}_{\perp}R_{\perp d} \, {}_{\perp}\bar{R}_{\perp d})}{\left(\frac{\partial F}{\partial \theta}\right)_{\theta=\theta_p} \, {}_{\parallel}\bar{R}_{\parallel d}} \, \frac{f_{\parallel}^2(0)}{f_{\parallel}^2(d)} \quad . \tag{7}$$

In the table, $|\lambda|$ is called EXTR MAG and ϕ is called EXTR ANG. The height was taken to be 56 km when generating the results of Table 4. More precisely, the excitation factor in equation (7) is for ground-based vertical electric dipole excitation of the vertical electric field at the ground. Thus the whispering gallery modes are weakly excited as are horizontally polarized modes relative to vertically polarized modes. The latter are expressed by the polarization magnitude and angle (in degrees) in the eighth and ninth columns of Table 4. The polarizations are calculated by using an equation given by Pappert.[19] Values greater than unity for the magnitude indicate principally vertically polarized (TM) waves, whereas magnitudes less than unity indicate principally horizontally polarized (TE) waves. It will be seen that the first eight modes contain comparable mixtures of TE and TM polarization. The higher order modes then divide into TE and TM sets, as evidenced by the magnitude of the polarization as well as the magnitude of the excitation factor. Observe how the angle of the polarization alternates between a large and small value. We have found this to be a typical behavior throughout the LF band and have found it useful in spotting potentially missing modes. In that regard the magnitude of the excitation factor as well as the magnitude of the polarization are also quite useful.

The remaining results in this section are for a 0.5 Gauss geomagnetic field, an azimuth of 45°, and a dip angle of 60°. Tables 5 and 7 show mode sets

for these geomagnetic conditions for the Deeks' and GE-TEMPO profiles. The tables apply to 150 kHz and, in particular, Table 5 applies to the Deeks' summertime day profile and Table 7 to the GE-TEMPO day profile. In each instance eighteen modes are shown. For the Deeks' profile the attenuation rates range between about 8.7 dB/Mm and 36 dB/Mm (just as they did for the geomagnetic conditions which apply to Table 4) whereas they range between about 11 dB/Mm and 46 dB/Mm for the GE-TEMPO profile. The additional loss for the GE-TEMPO profile, as explained previously, would be anticipated on the basis of its greater ionization above 64 km (see Figure 1). The consequences of the higher attenuation rates on mode sum plots are shown in Figures 5 through 7. Those curves show range plot comparisons for the Deeks' and GE-TEMPO profiles. Figure 5 is for a ground based transmitter and receiver, Figure 6 is for transmitter and receiver altitudes of 30 km and Figure 7 is for transmitter-receiver altitudes of 50 km. At the more distant ranges differences in excess of 10 dB occur. The thing most amazing to us, and unexplained, is the coincidence in the null and maxima locations for the two rather disparate profiles. The proliferation of mode structure with increasing altitude of the transmitter and receiver is evident, though the deepest nulls rather surprisingly occur for the transmitter-receiver altitude of 30 km. Picking up more of the whispering gallery modes with the transmitter-receiver combination at 50 km tends to fill in the deep nulls occurring with the 30 km combination.

All of the remaining results in this section are for the GE-TEMPO day profile. Tables 6 through 10 give the mode data sets at 100, 150, 200, 250 and 300 kHz. The number of modes range from a dozen at 100 kHz to 28 at 300 kHz. Minimum modal attenuation rates range from about 7.7 dB/Mm at 100 kHz to about 19 dB/Mm at 300 kHz. Mode spacing for the real part of the eigenangle

is generally comparable to or greater than a few hundredths of a degree and for the imaginary part of the eigenangle the mode spacing is generally comparable to or greater than a few thousandths of a degree. There can be exceptions however. The seventeenth and eighteenth modes for the 300 kHz case (Table 10) have real parts which differ by only 0.004° and have imaginary parts which are identical to the number of places printed out (i.e. to a thousandth of a degree). This points out the rigid demands on the program from the standpoint of eigenvalue resolution. It will also be noted from the tabulations that the excitation factors for the whispering gallery type modes show a monotonic decrease, unlike the behavior in Table 1, with frequency.

Figures 8 through 12 show range plots for frequencies of 100, 150, 200, 250 and 300 kHz. On each plot are curves for ground-to-ground transmission, for transmitter and receiver at 30 km and for transmitter and receiver at 50 km. The null in the ground-to-ground transmission curves which, depending upon frequency, falls in the range from about 800 to 1400 km is a manifestation of the ground wave and first hop sky wave interference null. Even up through 300 kHz the ground-to-ground curves show relatively little modal structure, indicating that only a few modes are required for that configuration. The mode structure is considerably more complicated for the elevated transmitter and receiver cases. On the basis of the mode picture this would be anticipated since whispering gallery type modes tend to become more influential with terminal elevation. On the basis of a wave hop picture the added structure would be anticipated since more multipath possibilities exist when the terminals are elevated. When the transmitter and receiver are on the ground, for example, only one path applies to a single ionospheric reflection. When the terminals are elevated, on the other hand, there exist four paths, or hops, linking transmitter and receiver which correspond to a

single ionospheric bounce. Though the absolute signal levels and the location of the nulls would be quite sensitive to the ionospheric model, the severity of multimode interference, depth of nulls, etc is probably quite realistically modeled by the results shown in Figures 8 through 12. Generally it will be observed that the deepest fades occur for the transmitter and receiver altitudes of 30 km. For ground-to-ground transmission the fact that whispering gallery modes do not play a role reduces the modal interference but at the same time also reduces the mean signal level. The 50 km to 50 km transmission link where the whispering gallery modes play their fullest role shows the largest signal strengths on the mean; but as the figures show, rather deep fades can be expected for that configuration as well.

Figures 13 through 17 show the height behavior of the total field for frequencies of 100 kHz, 150 kHz, 200 kHz, 250 kHz and 300 kHz. Each figure contains three curves. One is for a ground based transmitter, another is for a transmitter at 30 km and the third is for a transmitter at 50 km. All curves are for a range of 2 Mm. The first thing that is striking about these plots is the depth of the nulls that would be expected for the elevated transmitter cases. The altitude location of these nulls would be sensitive to the range as would be the absolute field strength at any given altitude. For the case selected (i.e. a range of 2 Mm), it is true that for all frequencies the strongest ground signal obtains with the ground based transmitter and that the strongest signal at 50 km results when the transmitter is at 50 km. It is true also, for the cases examined, that the ground based transmitter yields the lowest signal level at 50 km.

In addition to speedier techniques for determining the ionospheric reflection coefficients as well as more automated mode search capability, LF propagation may be better treated, especially under nighttime conditions, by

alternative methods. The wave hop method already mentioned is one such possibility. Another possibility would be something akin to the hybrid method of Felsen and coworkers, where a mixture of modes and hops are used to describe the field. The remainder of the section has been structured with that possibility in mind. In particular we will suggest a possible scheme for deciding on the modes to be included though we will leave for future study the treatment and inclusion of hops. For simplicity we also restrict the discussion to range considerations with the transmitter at the same altitude as the receiver.

Modes which are highly evanescent at the terminal locations contribute little to the mode sums. The degree of evanescence is determined roughly by the factor $\exp\left|-2/3(k/\alpha)(\alpha\ \Delta z)^{3/2}\right|$, where Δz is measured upwards from the terminal altitude. For the sake of argument let us say we require the degree of evanescence to be 20 dB. Then we require roughly that

$$8.68\ \left[\frac{2}{3}\ (k/\alpha)\ (\alpha\ \Delta z)^{3/2}\right] \simeq 20\ . \tag{7}$$

Taking 300 kHz for sample calculations, equation (7) gives

$$\Delta z \simeq 9.88\ \text{km}\ . \tag{8}$$

The condition that the wave just evolves into an evanescent stage at $z_o + \Delta z$, where z_o is the transmitter-receiver altitude, is

$$C_H^2 + \alpha\ (z_o + \Delta z - H) = 0\ . \tag{9}$$

The imaginary part of C_H is ignored in these estimates. From equation (9) we find for z_o = 0, 30, and 50 km the following (H was taken to be 55 km for all calculations involving the GE-TEMPO day profile);

$$\begin{aligned} z_o &= 0 \qquad \theta_r = 83.16° \\ z_o &= 30 \qquad \theta_r = 86.05° \\ z_o &= 50 \qquad \theta_r = 90° . \end{aligned} \tag{10}$$

The last of equation (10) is the interpretation for the real part of θ when C_H^2 given by equation (9) is negative. Equations (10) give the upper bound on the eigenangle search for the three transmitter receiver configurations. It is suggested that the lower bound be selected as follows: The hop calculations are most easily implemented when asymptotic expansions can be used for the modified Hankel functions of order one third. We thus determine the lower bound on C_H by requiring that

$$(k/\alpha)^{2/3} \left[C_H^2 + \alpha (z_o - H)\right] = 5 \tag{11}$$

The left-hand side of equation (11) is the argument of the Hankel functions of order one third, and the number 5 on the right hand side has, for the sake of example, been assumed sufficiently large relative to one to justify asymptotic expansions of the Hankel functions of order one third. Again the imaginary part of C_H is ignored in these estimates. From equation (11) we find

$$z_o = 0 \qquad \vartheta_r = 81.08°$$

$$z_o = 30 \qquad \vartheta_r = 83.05° \tag{12}$$

$$z_o = 50 \qquad \vartheta_r = 84.76° .$$

Combining the results from (10) and (12), the ranges over which modes would be located are

$$z_o = 0: \quad 81.08° \leq \vartheta_r \leq 83.16°: \quad \text{Modes } 17\text{-}28$$

$$z_o = 30: \; 83.05° \leq \vartheta_r \leq 86.05°: \quad \text{Modes } 5\text{-}18$$

$$z_o = 50: \; 84.76° \leq \vartheta_r \leq 90°: \quad \text{Modes } 1\text{-}8 .$$

Calculations based on these combinations are shown in Figures 18 through 20, where they are compared with the results of the full mode set.

The results for the limited mode set for the $z_o = 0$ case are indistinquishable from the results for the full modes set. This is because the lower limit 81.08° on θ_r is within the region of very lossy modes. As a matter of fact even the restricted mode range 17-28 includes many more modes than are necessary to adequately represent the $z_o = 0$ case. The disparity between the full and abbreviated mode set results for the cases $z_o = 30$ and 50 km points out the importance of higher order modes or hop contributions. Supplementing the restricted mode calculations with hops via the methods of Felsen and coworkers is an interesting possibility.

CONCLUSIONS

Waveguide calculations have been carried out throughout the LF band for a daytime ionospheric model. On the basis of the study it would appear feasible at the present time to perform case studies for additional daytime models as well as for PCA or artifically depressed ionospheres. Production runs, however, would depend upon the outcome of two developments: (1) Replacement of full-wave ionospheric reflection calculations by either phase integral methods or by a combination of phase integral and full-wave methods. (2) Improvement and automation of mode search techniques. MODESRCH[17] was found to have numerical difficulties at frequencies above about 150 kHz, and the TRACE routime of Ferguson[18] can switch without warning from tracing one factor of the modal equation to tracing the other. Very likely, too, the TRACE routine would totally miss modes over low conductivity terrain. Extension of calculational capability for nighttime ionospheres and into the MF band for both day and night ionospheres might require alternative methods. The wave hop[3-7] and "hybrid"[9-12] methods are two such possibilities.

Mode sums and height gains generated in this study point out the severity of fading to be expected, particularly in the upper LF band, when elevated transmitters and receivers are involved. For the prototype daytime ionospheres considered in this study, the number of modes ranged from a dozen at 100 kHz to 28 at 300 kHz. The results generated here should form a useful basis against which to compare results of alternative methods.

RECOMMENDATIONS

1. Improve mode search methods and simplify ionospheric full wave reflection calculations for application of waveguide methods to the upper LF band and above.

2. Investigate the utility of "hybrid" methods whereby fields are calculated by combining waveguide and wave hop methods.

Table 2.

GE-TEMPO Daytime Electron Density (N_e) and Collision Frequency (ν_e) Profiles

Altitude (km)	$N_e(cm^{-3})$	$\nu_e(s^{-1})$
50	4.27×10^{-1}	1.29×10^{8}
55	6.50	
60	8.43×10^{1}	
65	2.07×10^{2}	
70	5.72×10^{2}	
75	1.34×10^{3}	
80	2.80×10^{3}	9.99×10^{5}

Table 3

Deeks' Summertime Day Electron Density (N_e) and Collision Frequency (ν_e) Profiles

Altitude (km)	$N_e(cm^{-3})$	$\nu_e(s^{-1})$	Altitude (km)	$N_e(cm^{-3})$	$\nu_e(s^{-1})$
90.00	2.25+003	2×10^5	72.50	2.90+002	
89.50	1.65+003		72.00	2.45+002	
89.00	1.35+003		71.50	1.90+002	
88.50	1.20+003		71.00	1.60+002	
88.00	1.15+003		70.50	1.35+002	
87.50	1.05+003		70.00	1.20+002	
87.00	1.00+003		69.50	1.10+002	
86.50	9.60+002		69.00	1.00+002	
86.00	9.20+002		68.50	9.80+001	
85.50	8.90+002		68.00	9.60+001	1×10^7
85.00	8.60+002		67.50	9.70+001	
84.50	8.20+002		67.00	1.00+002	
84.00	8.00+002		66.50	1.10+002	
83.50	7.70+002		66.00	1.20+002	
83.00	7.40+002		65.50	1.35+002	
82.50	7.20+002		65.00	1.45+002	
82.00	7.00+002		64.50	1.60+002	
81.50	6.80+002		64.00	1.65+002	
81.00	6.60+002		63.50	1.75+002	
80.50	6.40+002		63.00	1.75+002	
80.00	6.20+002		62.50	1.70+002	
79.50	6.10+002		62.00	1.65+002	
79.00	5.90+002		61.50	1.55+002	
78.50	5.70+002		61.00	1.40+002	
78.00	5.50+002		60.50	1.20+002	
77.50	5.40+002		60.00	1.05+002	
77.00	5.20+002		59.50	8.30+001	
76.50	4.85+002		59.00	6.40+001	
76.00	4.75+002		58.50	4.60+001	
75.50	4.60+002		58.00	3.00+001	
75.00	4.40+002		57.50	1.85+001	
74.50	4.15+002		57.00	1.00+001	
74.00	3.90+002		56.50	5.44+000	
73.50	3.60+002		56.00	2.96+000	5×10^7
73.00	3.30+002				

REFERENCES

1. Roberts, C. R., D-layer whispering gallery propagation experiment, AFCRL LDF 5-71 prepared by General Electric Co. for Air Force Cambridge Research Laboratories, May 1973.

2. Videberg, J. I. and G. S. Sales, Long range survivable MF radio communication study using high altitude whispering gallery modes, Air Force Cambridge Research Laboratories report no. AFCRL-TR-0552, Aug 1973.

3. Wait, J. R., A diffraction theory of LF skywave propagation, J. Geophys. Res., 66, no. 6, 1713-1724, 1961.

4. Berry, L. A., Wave hop theory of long distance propagation of low frequency radio waves, Radio Sci., J. Res. NBS 68D, No. 12, 1275-1284, 1964.

5. Berry, L. A. and M. E. Chrisman, The path integrals of LF/VLF wave hop theory, Radio Sci., J. Res. NBS 69D, No. 11, 1469-1480, 1965.

6. Berry, L. A., G. Gonzalez and J. L. Lloyd, The wave hop series for an anisotropic ionosphere, Radio Sci., 4, 1025-1027, 1969.

7. Berry, L. A. and J. E. Herman, A wave hop propagation program for an anisotropic ionosphere, OT/ITS Research Report 11 Office of Telecommunications, Boulder, CO, 1971.

8. Campbell, P. H. M. and T. B. Jones, Low frequency radio propagation at high latitudes, IEEE Conference Publication No. 169 Antennas and Propagation, 47-50, 1978.

9. Ishihara, T. and L. B. Felsen, High frequency fields excited by a line source on a prefectly conducting concave cylindrical boundary, IEEE Trans. on Antennas and Propagation, vol. AP-26, 757-767, 1978.

10. Ishihara, T. and L. B. Felsen, High frequency fields excited by a line source on a concave cylindrical impedance surface, IEEE Trans. on Antennas and Propagation, vol. AP-27, 172-179, 1979.

11. Felsen, L. B. and T. Ishihara, Hybrid ray-mode formulation of ducted propagation, J. Acoust. Soc. Am., 65, 595-607, 1979.

12. Felsen, L. B., Propagation along concave surfaces, IEEE 1979 International Symposium Digest, Antennas and Propagation, Dec. 1979.

13. Pappert, R. A., W. F. Moler and L. R. Shockey, A FORTRAN program for waveguide propagation which allows for both vertical and horizontal dipole excitation, Interim Report No. 702 prepared by the Naval Electronics Laboratory Center (now NOSC) for the Defense Atomic Support Agency (now DNA), June 1970.

14. Pappert, R. A. and L. R. Shockey, WKB mode summing programs for VLF/ELF antennas of arbitrary length, shape and elevation, Interim Report No. 713 prepared by the Naval Electronics Laboratory Center (now NOSC) for the Defense Atomic Support Agency (now DNA), June 1971.

15. Deeks, D. G., D-region electron distributions in middle latitudes deduced from the reflection of long radio waves, Proc. Roy. Soc. A291, 1966, 413-437.

16. Knapp, W., Reaction rate, collision frequency and ambient ionospheric models for use in studies of radio propagation for nuclear environment. TEMPO report 66 TMP-82, General Electric, March 1967.

17. Morfitt, D. B. and C. H. Shellman, "MODESRCH", an improved computer program for obtaining ELF/VLF/LF mode constants in an earth-ionosphere waveguide, Naval Electronics Laboratory Center (now NOSC), Interim Report no. 77T prepared for the Defense Nuclear Agency, Oct. 1976.

18. Ferguson, J. A., An aid for using the NELC WAVEGUID program, NELC technical note 2480, Sep 1973.

19. Pappert, R. A., A numerical study of VLF mode structure and polarization below an anisotropic ionosphere, Radio Sci., 3, 3, 219-233, 1968.

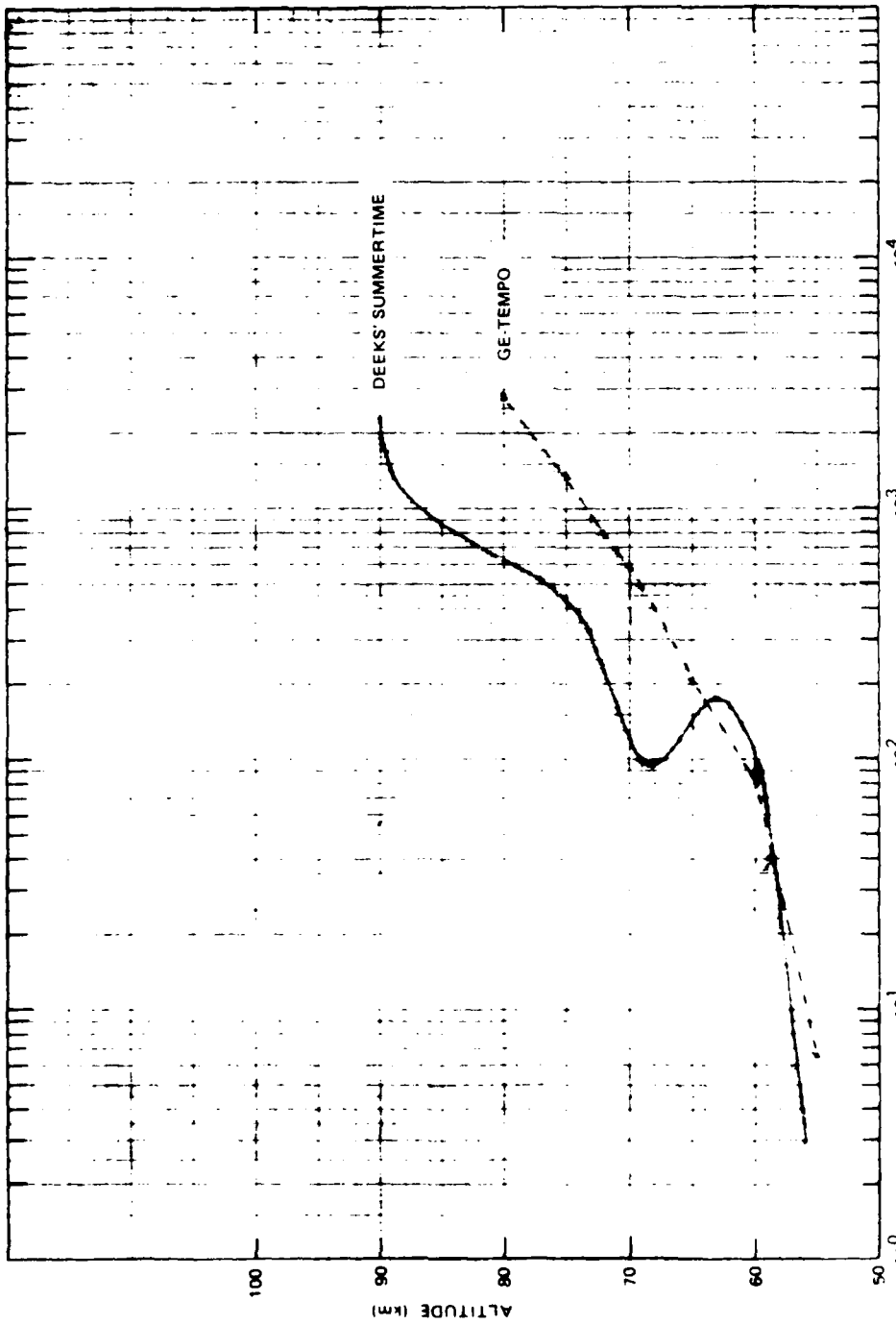

Figure 1. GE-TEMPO (dashed) and Deeks' summertime (solid) electron density profiles.

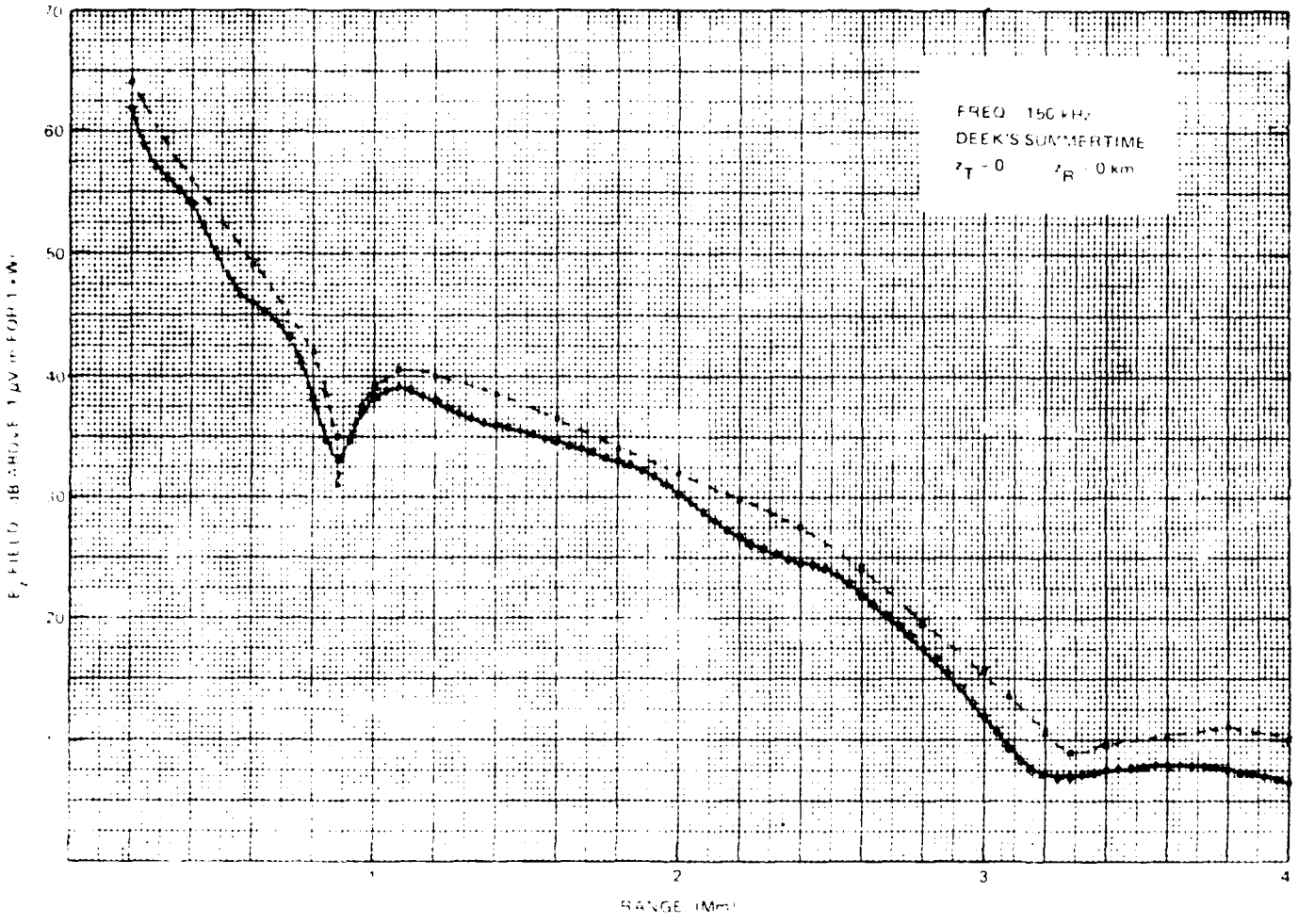

Figure 2. Waveguide (solid) and wave hop (dash-D) comparisons at 150 kHz for Deek's summertime day profile. Transmitter and receiver altitude = 0 km.

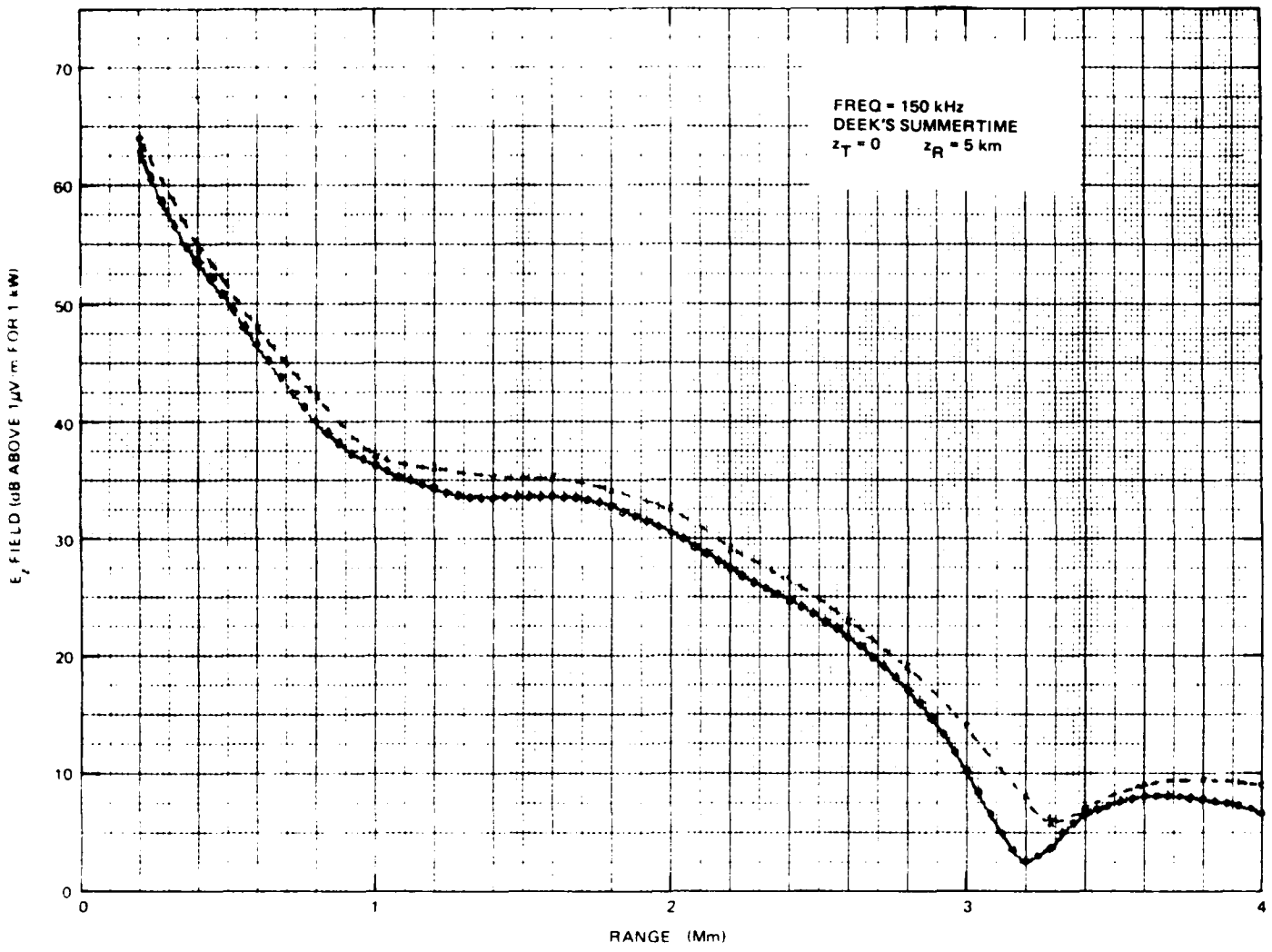

Figure 3. Waveguide (solid) and wave hop (dashed) comparisons at 150 kHz for Deeks' summertime day profile. Transmitter altitude = 0 km, receiver altitude = 5 km.

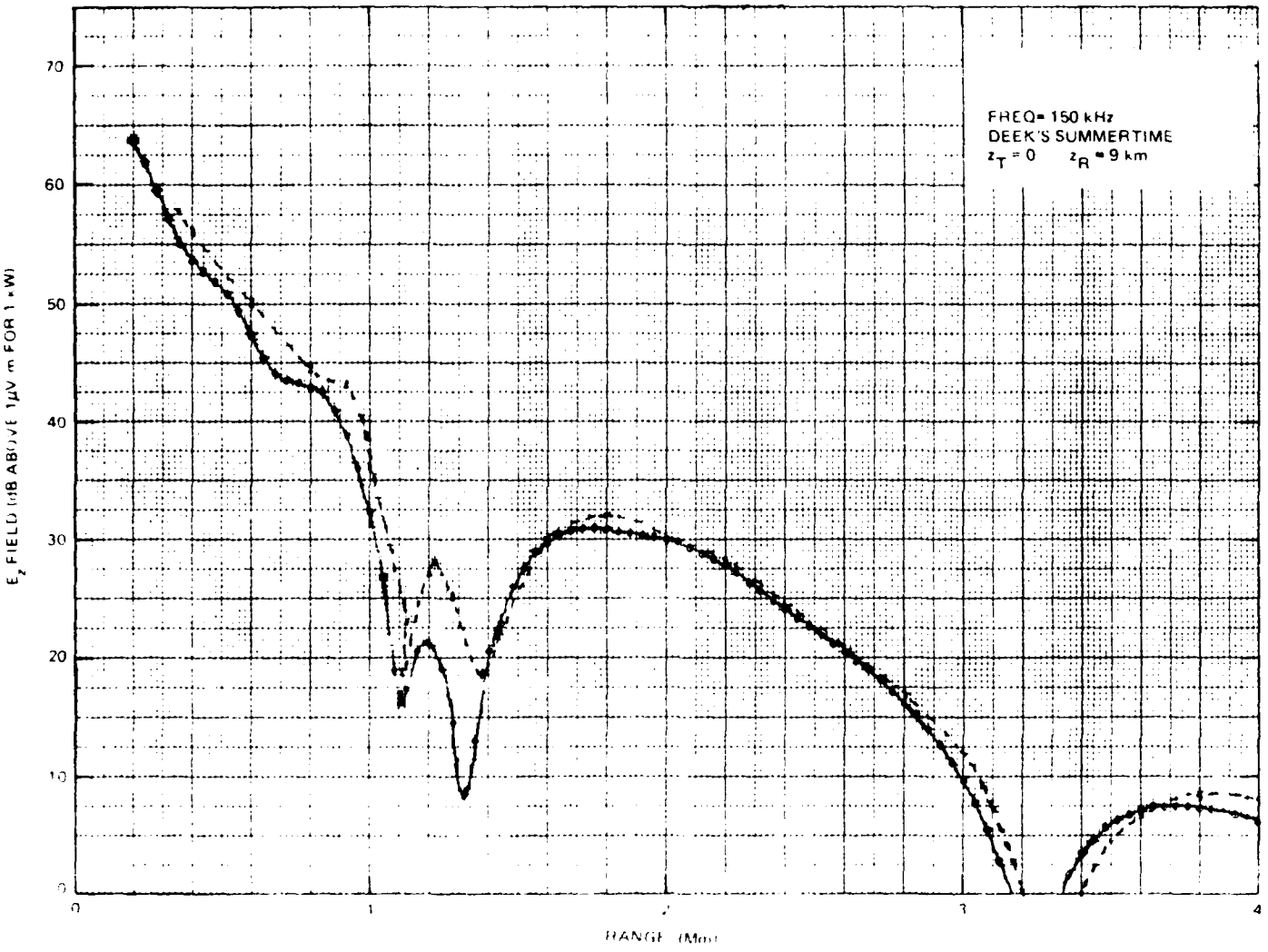

Figure 4. Waveguide (solid) and wave hop (dashed) comparisons at 150 kHz for Deeks' summertime day profile. Transmitter altitude = 0 km, receiver altitude = 9 km.

Table 4. Mode constants for Deeks' profile (150 kHz).
Azimuth = 0°, dip = 65.82°, B = 0.4508 gauss.

EXACT ***

MODE	REAL	IMAG	ATTEN	VOVERC	EXTR MAG	EXTR ANG	POL-MAG	POL-ANG
1	86.587	-.304	8.689	.99296	.2748-012	3.399	1.083	270.85
2	86.560	-.329	9.499	.99298	.6012-012	2.952	1.186	58.25
3	85.104	-.225	9.234	.99483	.6372-009	3.224	1.099	270.36
4	85.084	-.243	10.028	.99486	.6288-009	2.834	1.182	59.97
5	84.160	-.198	9.700	.99637	.5740-006	3.052	1.119	270.16
6	84.142	-.213	10.475	.99640	.8567-006	2.679	1.169	61.24
7	83.436	-.184	10.094	.99774	.5133-004	2.904	1.362	271.95
8	83.419	-.198	10.893	.99778	.1751-004	2.384	.982	58.24
9	82.857	-.158	9.476	.99896	.7506-003	2.275	7.498	246.89
10	82.809	-.201	12.096	.99906	.1275-004	2.179	.223	69.67
11	82.409	-.174	11.022	.99997	.9311-002	1.695	20.371	170.40
12	82.197	-.239	15.626	1.00046	.0705-004	2.452	.092	29.59
13	81.843	-.253	17.262	1.00133	.7695-002	1.526	16.823	146.89
14	81.525	-.297	21.023	1.00214	.3044-005	2.421	.088	17.81
15	81.157	-.321	23.751	1.00312	.4841-002	1.557	14.734	149.07
16	80.794	-.361	27.762	1.00412	.5395-005	2.255	.096	11.20
17	80.408	-.390	31.274	1.00524	.3319-002	1.590	13.770	156.05
18	80.020	-.431	35.939	1.00641	.7616-005	2.067	.104	6.52

Table 5. Mode constants for Deeks' profile (150 kHz).
Azimuth = 45°, dip = 60°, B = 0.5 gauss.

EXACT ***

MODE	REAL	IMAG	ATTEN	VOVERC	EXTR MAG	EXTR ANG	POL-MAG	POL-ANG
1	86.587	-.304	8.687	.99295	1.4236-012	3.405	.971	276.33
2	86.562	-.327	9.429	.99298	1.4514-012	2.853	.876	57.39
3	85.105	-.225	9.234	.99463	5.0906-009	3.261	.981	276.33
4	85.086	-.242	9.963	.99486	5.1411-009	2.711	.872	59.41
5	84.161	-.198	9.703	.99637	1.7103-006	3.090	.994	276.61
6	84.143	-.212	10.414	.99640	1.6743-006	2.591	.862	61.26
7	83.436	-.184	10.088	.99774	1.6893-004	2.914	1.212	279.13
8	83.420	-.197	10.849	.99777	1.0583-004	2.285	.719	58.56
9	82.858	-.158	9.428	.99896	5.7375-003	2.282	6.577	254.13
10	82.809	-.201	12.117	.99906	1.8359-004	2.088	.167	51.12
11	82.410	-.172	10.948	.99996	1.9443-002	1.691	17.558	178.55
12	82.197	-.240	15.663	1.00046	9.5017-005	2.364	.070	31.83
13	81.844	-.252	17.156	1.00133	1.7631-002	1.531	14.539	154.10
14	81.525	-.297	21.057	1.00214	8.2446-005	2.339	.068	20.87
15	81.158	-.320	23.626	1.00311	1.4779-002	1.562	13.012	156.08
16	80.794	-.361	27.769	1.00412	8.3795-005	2.205	.075	14.77
17	80.409	-.388	31.109	1.00524	1.3337-002	1.591	12.439	160.96
18	80.021	-.431	35.925	1.00641	8.6942-005	2.078	.084	9.36

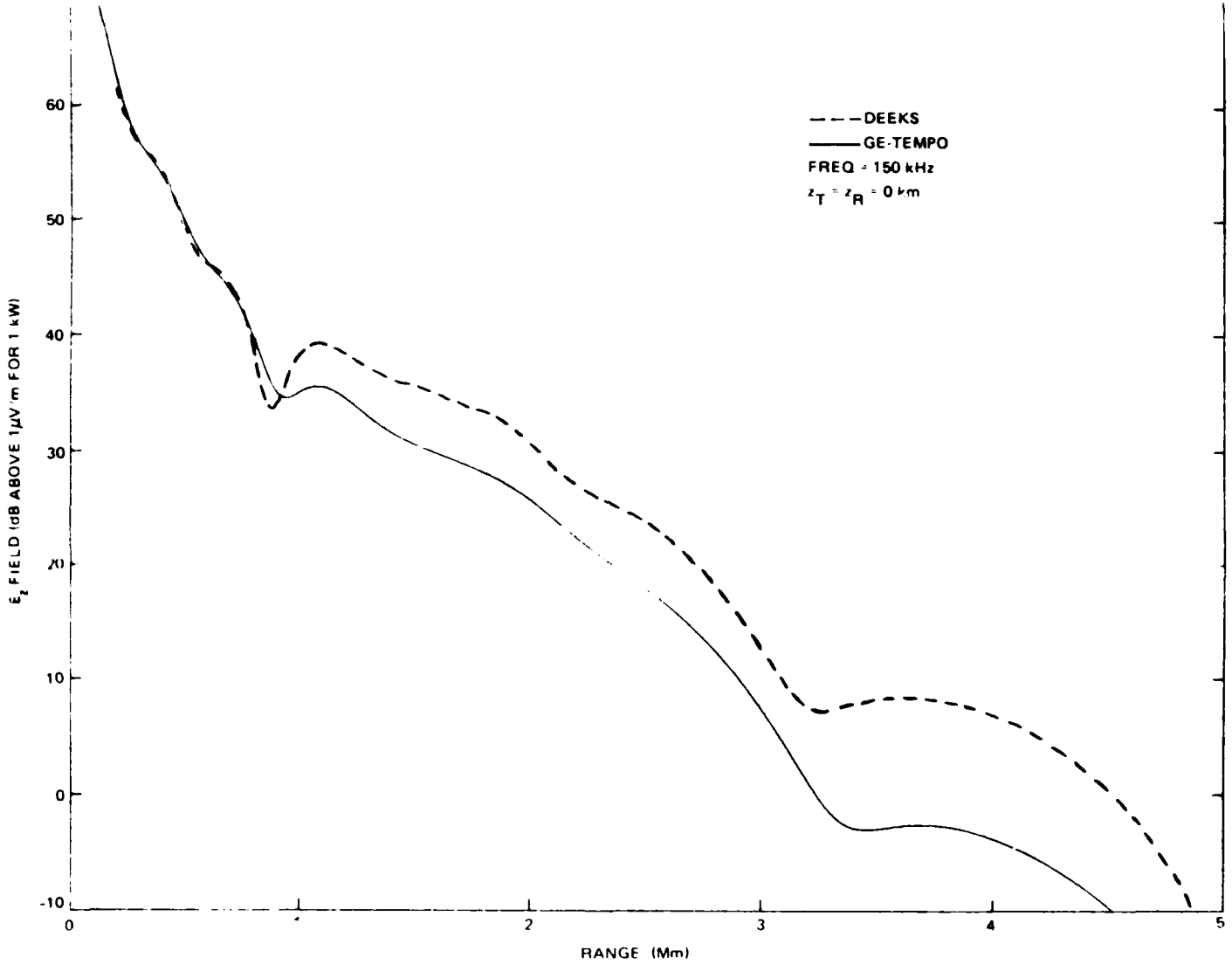

Figure 5. Waveguide comparisons for Deeks' (dashed) and GE-TEMPO (solid) profiles (150 kHz). Transmitter and receiver altitudes = 0 km.

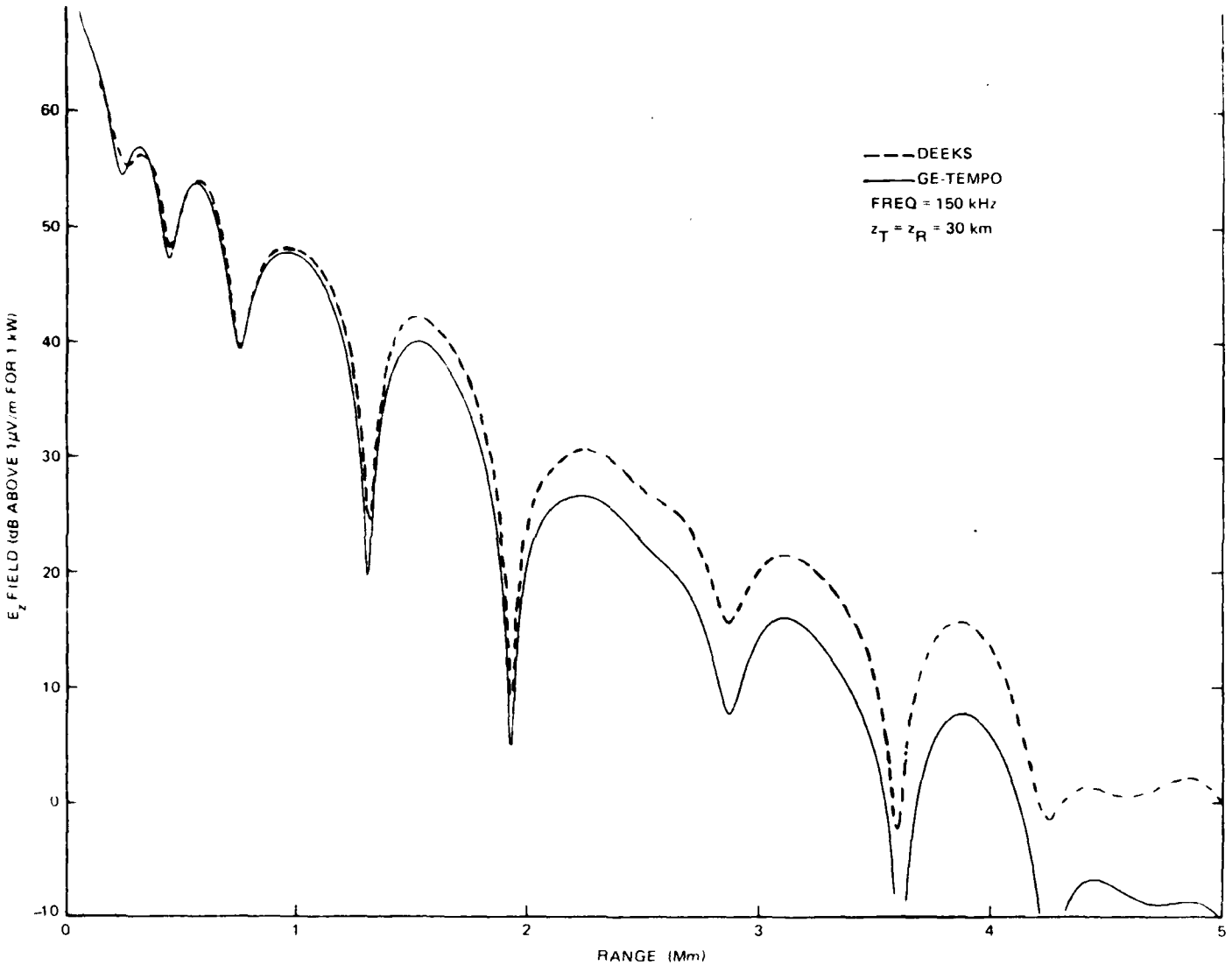

Figure 6. Waveguide comparisons for Deeks' (dashed) and GE-TEMPO profiles (150 kHz). Transmitter and receiver altitudes = 30 km.

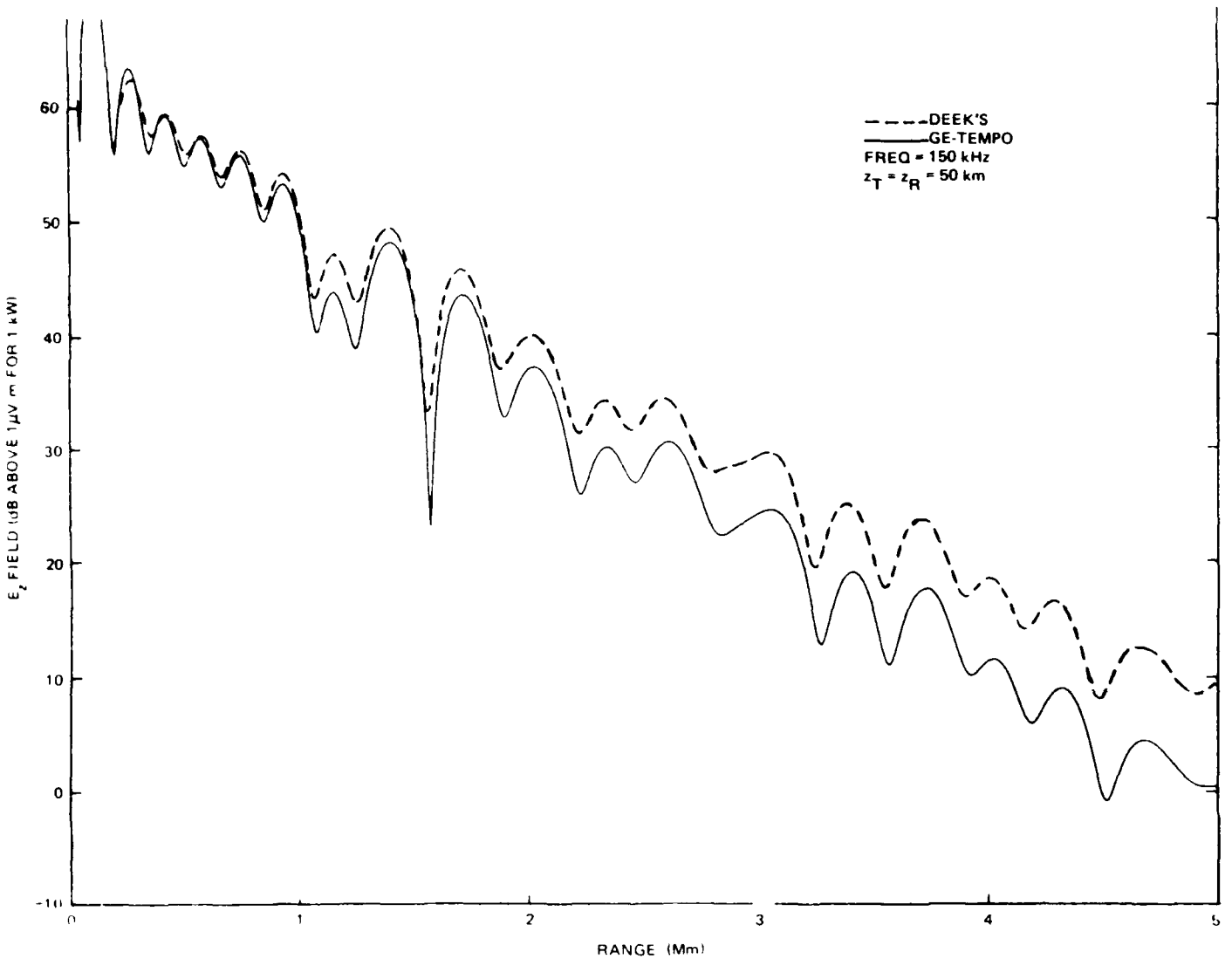

Figure 7. Waveguide comparisons for Deeks' (dashed) and GE-TEMPO (solid) profiles (150 kHz). Transmitter and receiver altitudes = 50 km.

Table 6. Mode constants for GE-TEMPO profile (100 kHz).

EXACT ***

MODE	REAL	IMAG	ATTEN	VOVERC	EXTR MAG	EXTR ANG	POL-MAG	POL-ANG
1	86.098	-.335	7.310	.99365	3.2124-008	3.132	.990	279.75
2	86.065	-.368	8.097	.99369	2.6907-008	2.453	.731	53.44
3	84.403	-.248	7.743	.99610	2.5035-005	2.932	1.040	280.49
4	84.377	-.273	8.566	.99615	1.8588-005	2.249	.691	56.18
5	83.333	-.205	7.617	.99811	2.8279-003	2.397	2.883	267.19
6	83.293	-.250	9.365	.99819	3.0544-004	2.048	.269	56.23
7	82.616	-.187	7.718	.99965	2.1952-002	1.785	13.299	188.42
8	82.346	-.295	12.583	1.00026	1.6968-004	2.527	.074	40.05
9	81.802	-.301	13.774	1.00159	2.4188-002	1.548	11.139	149.81
10	81.317	-.388	18.751	1.00284	1.7103-004	2.572	.074	27.74
11	80.756	-.411	21.165	1.00438	1.9966-002	1.574	8.306	151.22
12	80.191	-.500	27.311	1.00603	2.3897-004	2.443	.090	23.39

Table 7. Mode constants for GE-TEMPO profile (150 kHz).

—EXACT ***—

MODE	REAL	IMAG	ATTEN	VOVERC	EXTR MAG	EXTR ANG	POL-MAG	POL-ANG
1	86.772	-.378	10.367	.99296	1.5718-012	3.660	.991	281.18
2	86.696	-.411	11.388	.99299	1.3652-012	3.161	.721	62.98
3	85.220	-.280	11.214	.99481	5.2974-009	3.529	1.012	282.41
4	85.190	-.304	12.243	.99485	4.4193-009	3.034	.704	66.18
5	84.266	-.249	11.957	.99634	1.7396-006	3.360	1.033	283.63
6	84.237	-.269	12.965	.99639	1.3886-006	2.857	.689	68.84
7	83.536	-.233	12.589	.99770	1.5219-004	3.193	1.156	287.96
8	83.508	-.250	13.613	.99775	9.9840-005	2.565	.632	66.62
9	82.947	-.202	11.908	.99892	5.5026-003	2.550	4.213	283.80
10	82.898	-.256	15.212	.99902	3.9600-004	1.756	.240	44.01
11	82.507	-.213	13.324	.99990	1.9580-002	1.753	10.688	203.51
12	82.292	-.306	19.739	1.00039	2.7470-004	1.871	.113	27.30
13	81.952	-.314	21.107	1.00121	1.7470-002	1.521	7.474	179.98
14	81.623	-.380	26.621	1.00203	2.8654-004	1.727	.114	15.13
15	81.274	-.403	29.379	1.00295	1.4511-002	1.569	5.788	190.65
16	80.888	-.464	35.327	1.00400	3.7959-004	1.245	.136	2.32
17	80.528	-.504	39.839	1.00503	1.3207-002	1.653	4.418	217.01
18	80.083	-.556	46.042	1.00635	6.0310-004	.086	.165	335.19

Table 8. Mode constants for GE-TEMPO profile (200 kHz).

EXACT ***

MODE	REAL	IMAG	ATTEN	VOVERC	EXTR MAG	EXTR ANG	POL-MAG	POL-ANG
1	87.141	-.417	13.331	.99257	1.5034-017	4.230	.987	282.11
2	87.101	-.449	14.560	.99260	1.3634-017	3.845	.720	67.99
3	85.744	-.309	14.703	.99409	6.5076-013	4.157	1.010	283.82
4	85.712	-.332	15.911	.99413	5.8447-013	3.759	.704	70.99
5	84.870	-.276	15.821	.99534	6.0331-010	4.053	1.031	285.28
6	84.838	-.294	16.938	.99539	5.3068-010	3.633	.695	75.63
7	84.203	-.259	16.780	.99645	1.3371-007	3.889	1.050	286.58
8	84.170	-.272	17.722	.99651	1.1696-007	3.472	.691	76.43
9	83.650	-.249	17.621	.99748	1.0670-005	3.707	1.073	288.21
10	83.618	-.257	18.297	.99754	8.9949-006	3.214	.694	78.94
11	83.170	-.240	18.278	.99844	4.2948-004	3.608	1.215	301.30
12	83.141	-.245	18.747	.99850	2.9717-004	2.671	.697	67.38
13	82.763	-.201	16.251	.99932	9.1231-003	2.549	6.836	309.53
14	82.710	-.261	21.192	.99943	4.1279-004	.805	.233	16.97
15	82.442	-.236	19.866	1.00005	1.8189-002	1.644	11.403	232.81
16	82.249	-.304	26.254	1.00049	2.2187-004	.475	.121	355.64
17	81.993	-.321	28.666	1.00111	1.4614-002	1.492	9.217	239.28
18	81.733	-.351	32.312	1.00176	1.2228-004	5.914	.092	332.52

Table 9. Mode constants for GE-TEMPO profile (250 kHz).

EXACT ***

MODE	REAL	IMAG	ATTEN	VOVERC	EXTR MAG	EXTR ANG	POL-MAG	POL-ANG
1	87.438	-.455	16.291	.99233	5.2629-022	4.789	.985	282.75
2	87.395	-.487	17.719	.99235	4.9318-022	4.482	.719	71.15
3	86.125	-.336	18.214	.99362	1.3003-017	4.825	1.009	284.84
4	86.090	-.358	19.575	.99366	1.2425-017	4.514	.705	73.90
5	85.307	-.299	19.630	.99469	1.1632-013	4.747	1.030	286.51
6	85.273	-.315	20.789	.99473	1.0891-013	4.394	.702	76.39
7	84.682	-.279	20.697	.99564	5.9899-011	4.626	1.051	297.70
8	84.649	-.288	21.494	.99569	5.6601-011	4.193	.711	79.23
9	84.162	-.264	21.528	.99652	1.1435-008	4.406	1.075	288.73
10	84.132	-.266	21.819	.99658	1.0867-008	3.970	.732	82.97
11	83.708	-.252	22.118	.99736	9.9462-007	4.144	1.110	299.48
12	83.683	-.248	21.840	.99741	8.5289-007	3.683	.769	87.81
13	83.303	-.239	22.347	.99817	3.9876-005	3.806	1.131	292.35
14	83.285	-.231	21.656	.99820	3.5621-005	3.392	.869	91.93
15	82.931	-.226	22.249	.99895	3.9330-004	5.105	.590	339.72
16	82.930	-.213	20.986	.99895	1.8344-003	3.004	2.605	45.08
17	82.644	-.176	18.064	.99959	1.2198-002	2.212	39.730	325.65
18	82.577	-.236	24.431	.99973	3.1580-005	5.796	.093	348.17
19	82.365	-.223	23.703	1.00022	1.5260-002	1.489	131.120	252.84
20	82.203	-.260	28.304	1.00061	2.6424-006	1.514	.045	349.58
21	81.992	-.268	29.861	1.00112	1.1690-002	1.438	63.310	124.20
22	81.792	-.286	32.732	1.00161	1.2453-005	2.310	.038	1.51
23	81.572	-.295	34.634	1.00217	1.0021-002	1.499	24.166	139.69
24	81.358	-.310	37.370	1.00274	2.1112-005	2.231	.045	9.52

Table 10. Mode constants for GE-TEMPO profile (300 kHz).

EXACT ***

MODE	REAL	IMAG	ATTEN	VOVERC	EXTR MAG	POL-MAG	POL-ANG
1	87.670	-.493	19.258	.99215	1.6511-026	.983	283.21
2	87.624	-.524	20.870	.99218	1.6375-026	.710	73.39
3	86.423	-.362	21.712	.99328	8.2716-022	1.008	285.54
4	86.386	-.383	23.203	.99332	8.4011-022	.706	75.79
5	85.647	-.316	23.237	.99422	3.5018-018	1.029	287.18
6	85.613	-.331	24.362	.99426	3.6381-018	.713	78.04
7	85.050	-.291	24.170	.99506	3.1419-015	1.065	288.30
8	85.020	-.296	24.719	.99511	3.8708-015	.740	81.11
9	84.550	-.270	24.678	.99586	6.8257-012	1.088	288.68
10	84.526	-.268	24.570	.99590	6.3495-012	.791	85.18
11	84.115	-.250	24.689	.99661	1.2654-009	1.144	288.64
12	84.099	-.245	24.189	.99664	1.1436-009	.892	90.19
13	83.730	-.230	24.194	.99732	1.0728-007	1.234	287.13
14	83.721	-.226	23.720	.99734	1.0783-007	1.103	94.15
15	83.386	-.212	23.510	.99800	4.2162-006	1.296	281.56
16	83.380	-.210	23.314	.99801	5.1475-006	1.491	82.80
17	83.071	-.197	22.852	.99865	1.3234-004	1.171	302.58
18	83.067	-.197	22.819	.99866	1.9277-004	1.553	35.56
19	82.788	-.172	20.762	.99927	3.2919-003	10.813	310.46
20	82.779	-.196	23.672	.99928	5.7465-005	.173	8.35
21	82.568	-.157	19.567	.99976	1.3154-002	36.977	224.12
22	82.489	-.210	26.360	.99994	3.2068-005	.066	14.21
23	82.318	-.204	26.201	1.00034	1.2523-002	24.655	175.58
24	82.177	-.233	30.477	1.00067	2.9126-005	.054	9.62
25	82.006	-.239	31.993	1.00108	9.9931-003	19.692	179.15
26	81.841	-.[illegible]	35.086	1.00149	2.8507-005	.057	4.68
27	81.665	-.267	37.151	1.00194	8.5178-003	19.283	186.25
28	81.487	-.281	40.047	1.00240	2.5991-005	.061	359.98

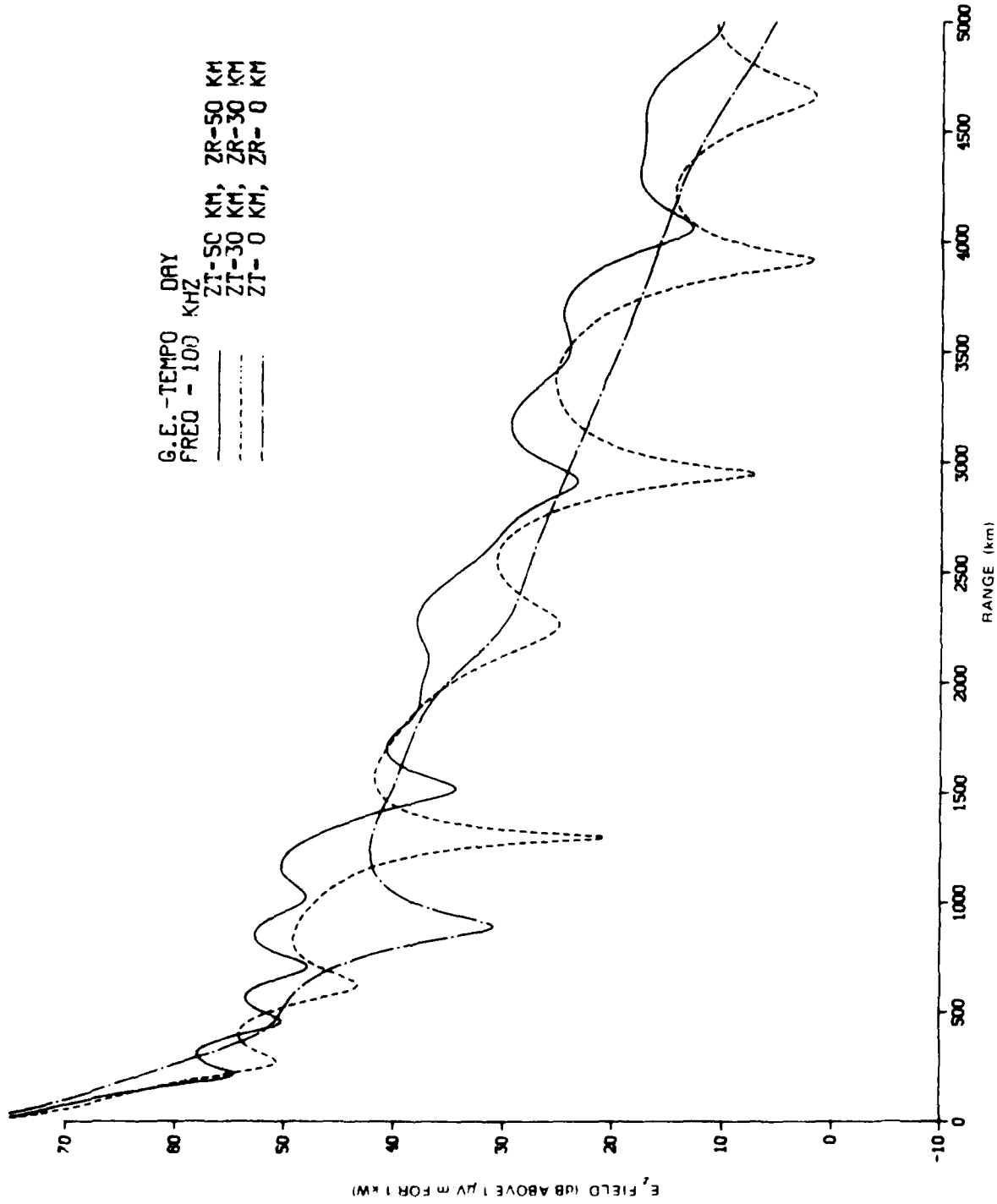

Figure 8. Range plots for GE-TEMPO day (100 kHz).

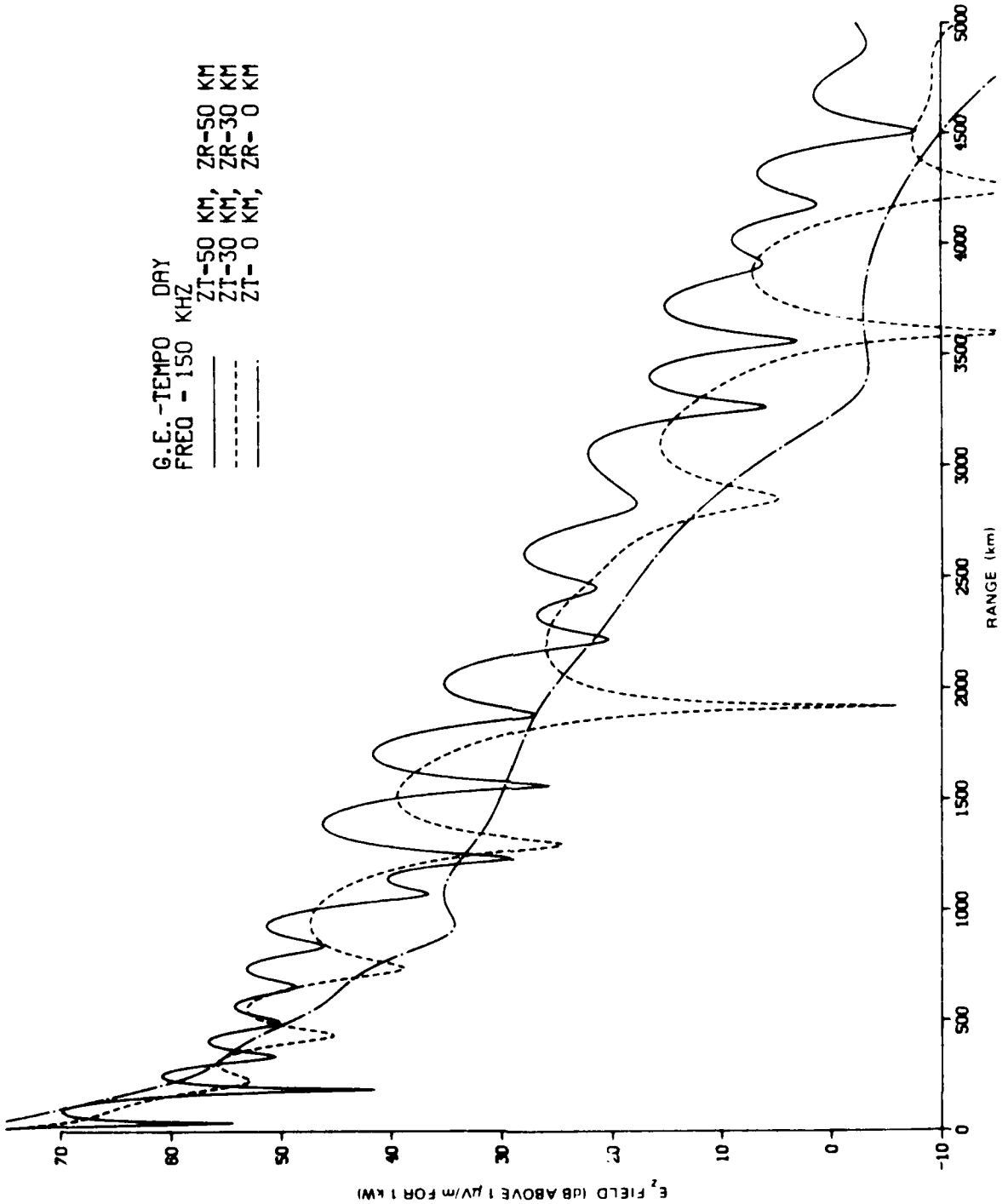

Figure 9. Range plots for GE-TEMPO day (150 kHz).

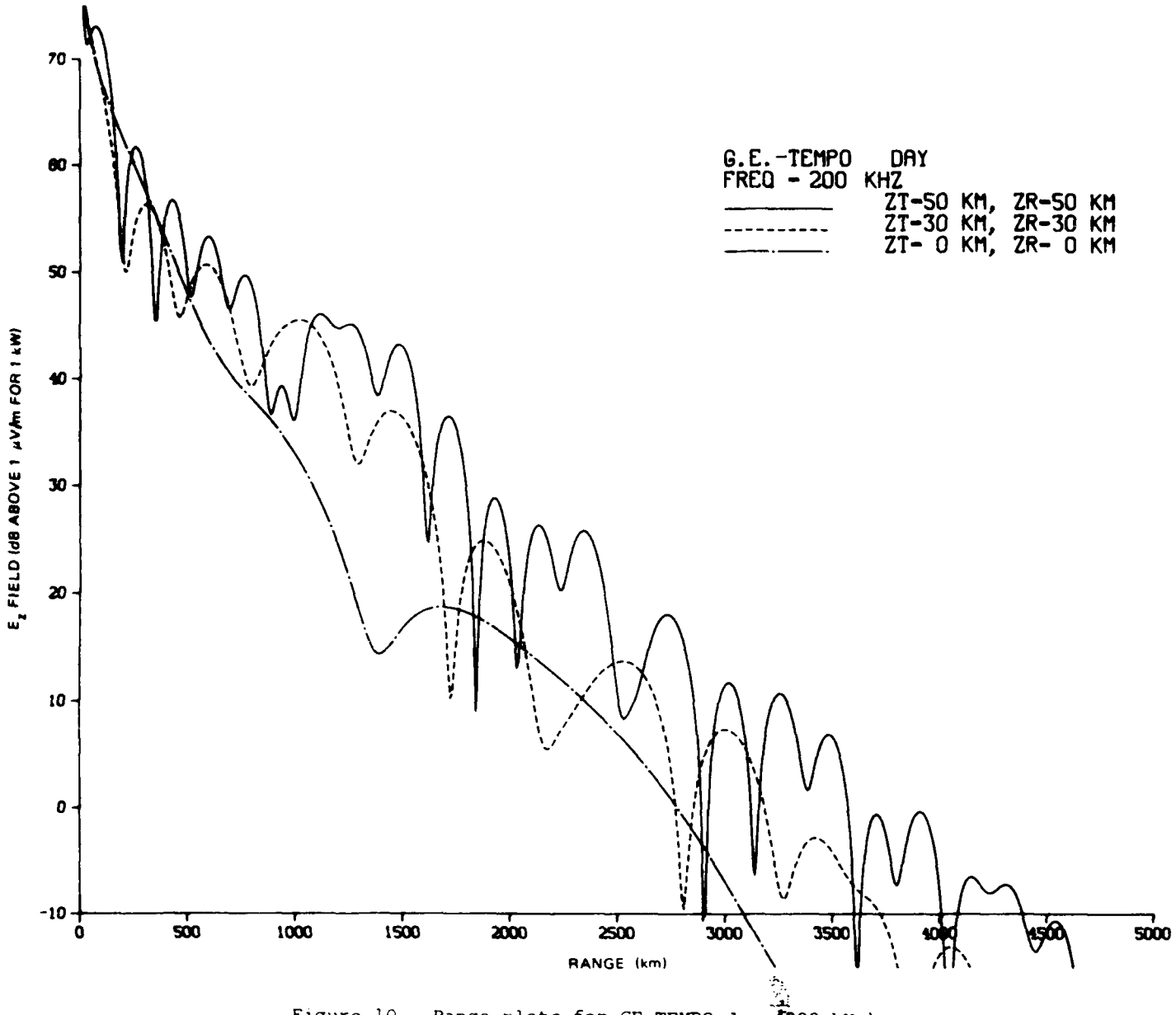

Figure 10. Range plots for GE-TEMPO day (200 kHz).

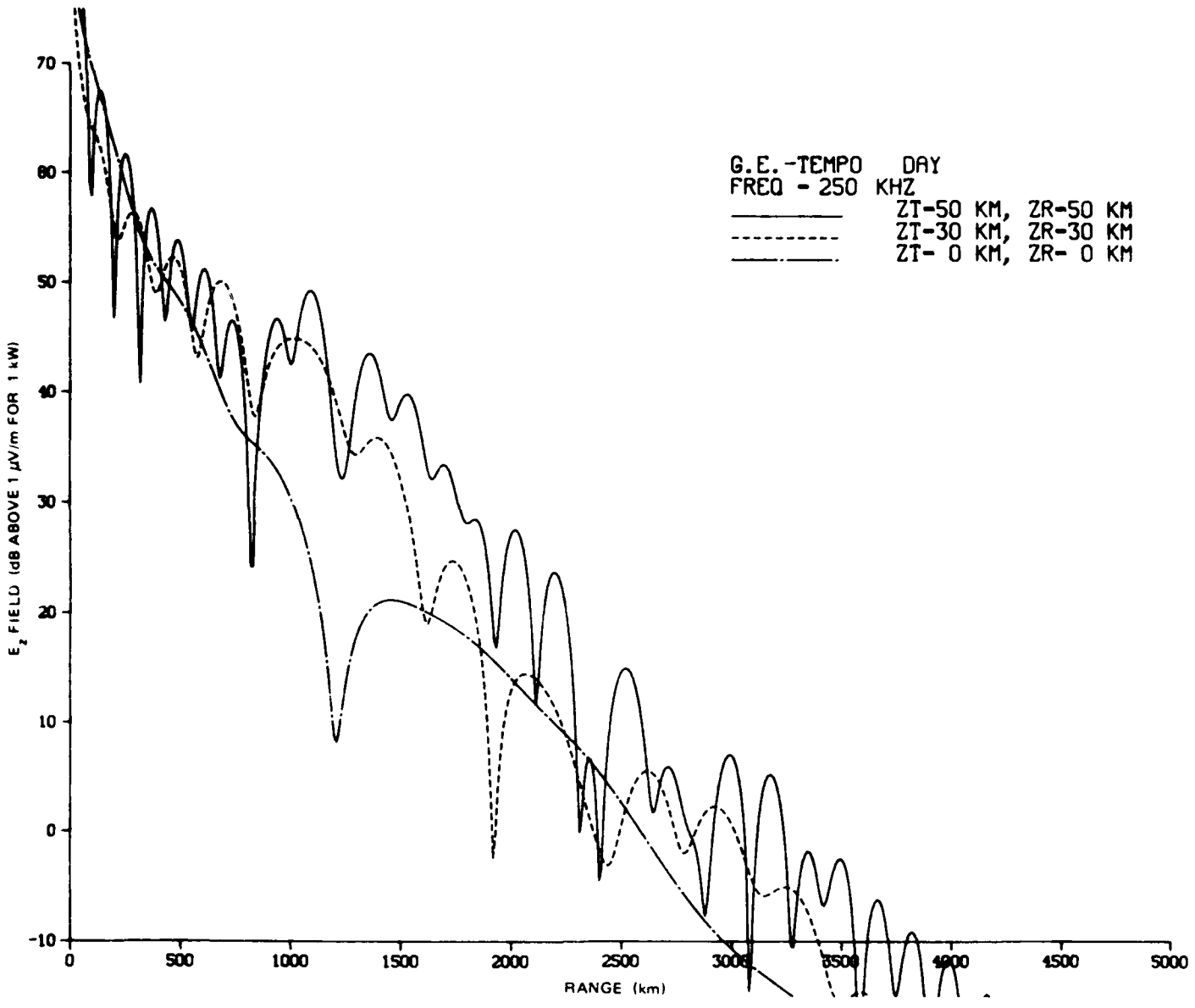

Figure 11. Range plots for GE-TEMPO day (250 kHz).

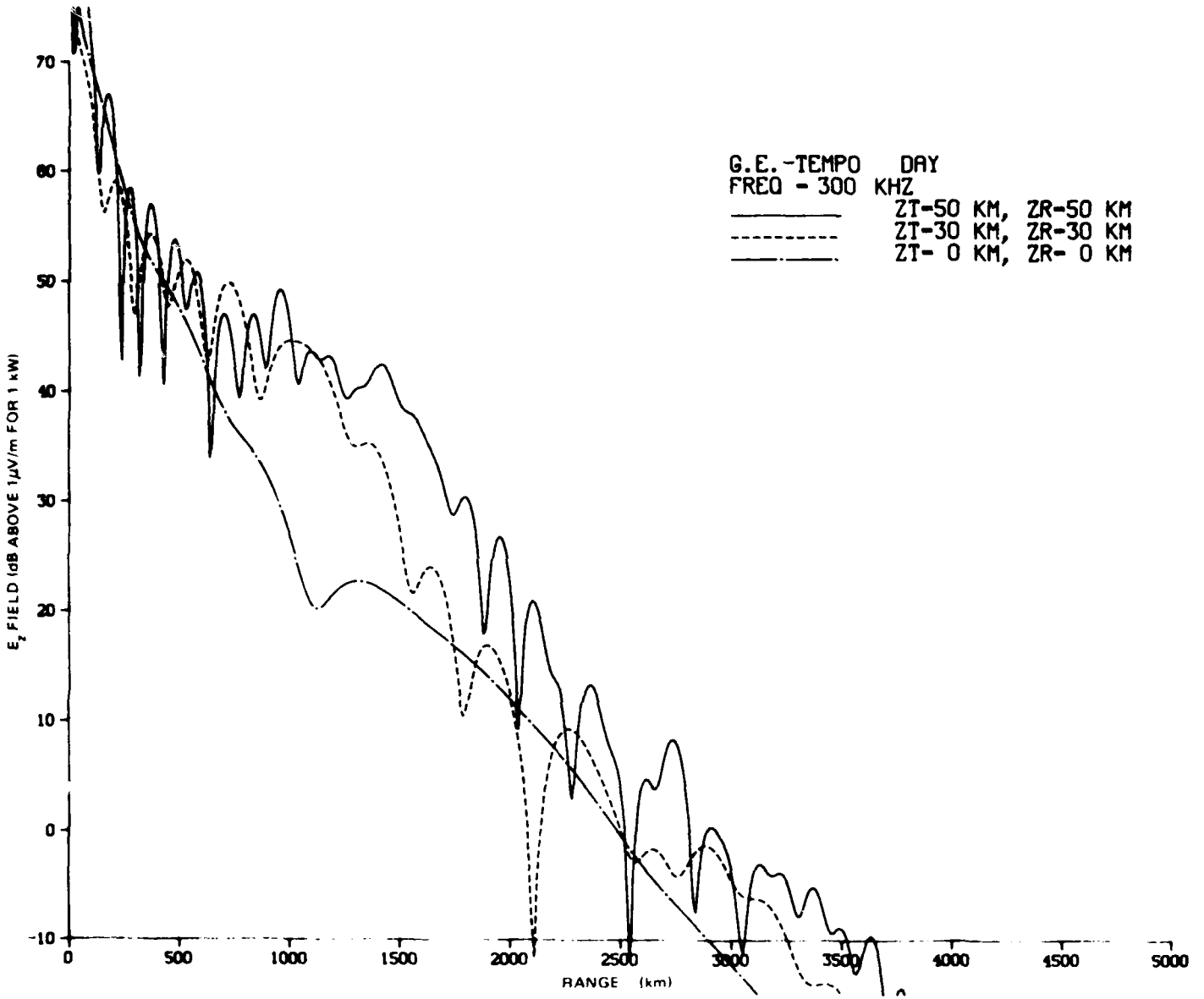

Figure 12. Range plots for GE-TEMPO day (300 kHz).

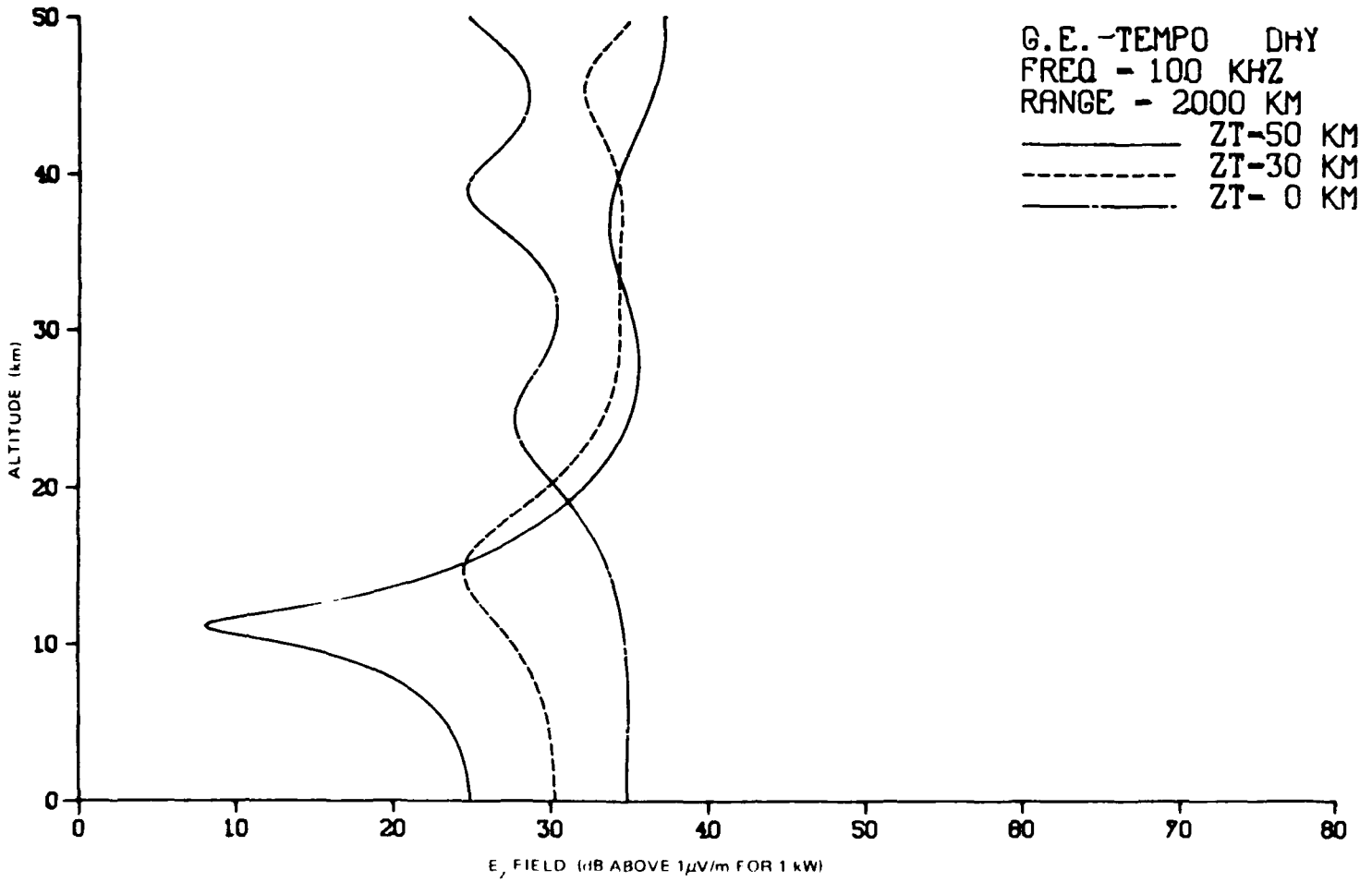

Figure 13. E_z as a function of height for GE-TEMPO day (100 kHz).

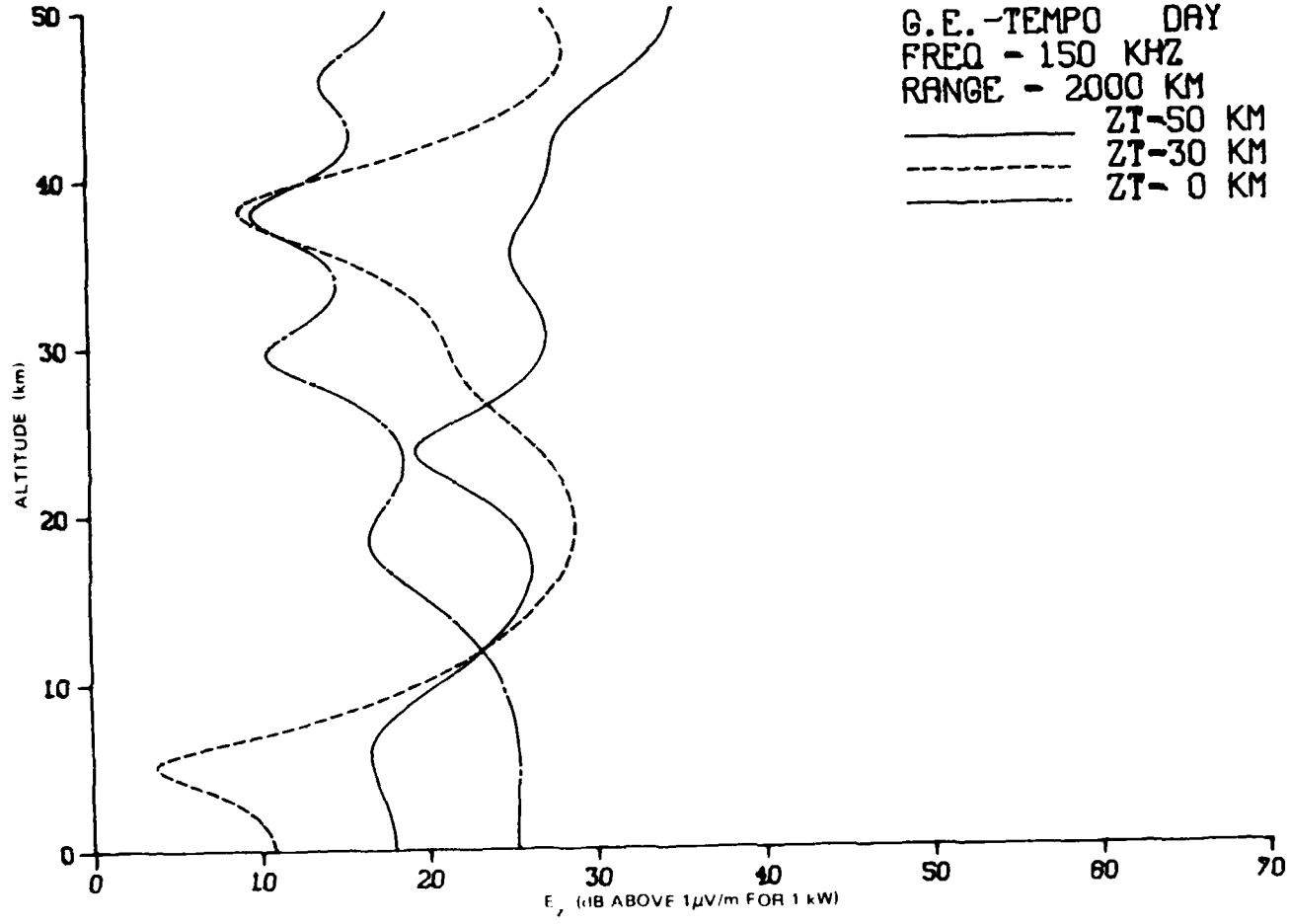

Figure 14. E_z as a function of height for GE-TEMPO day (150 kHz).

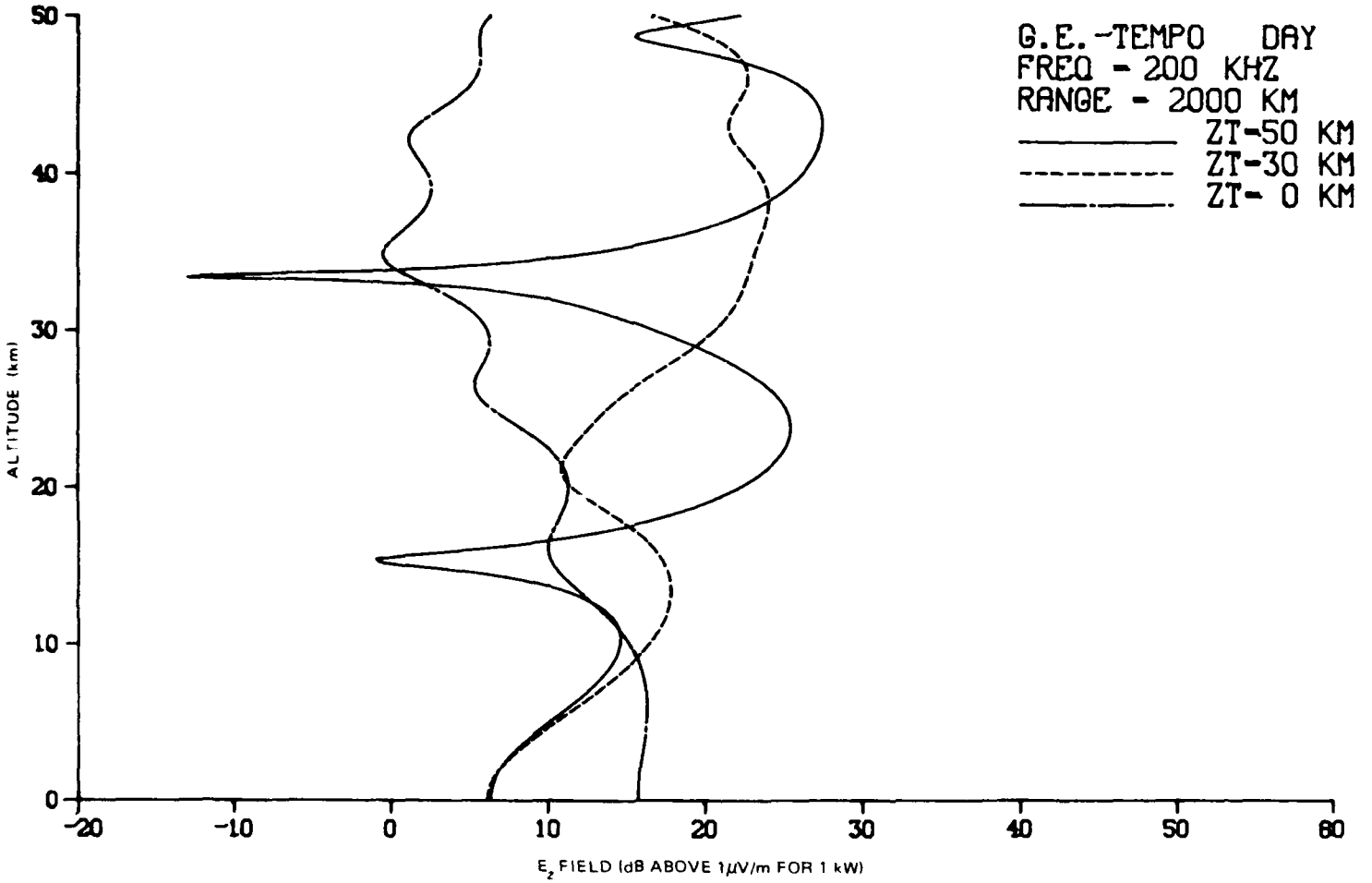

Figure 15. E_z as a function of height for GE-TEMPO day (200 kHz).

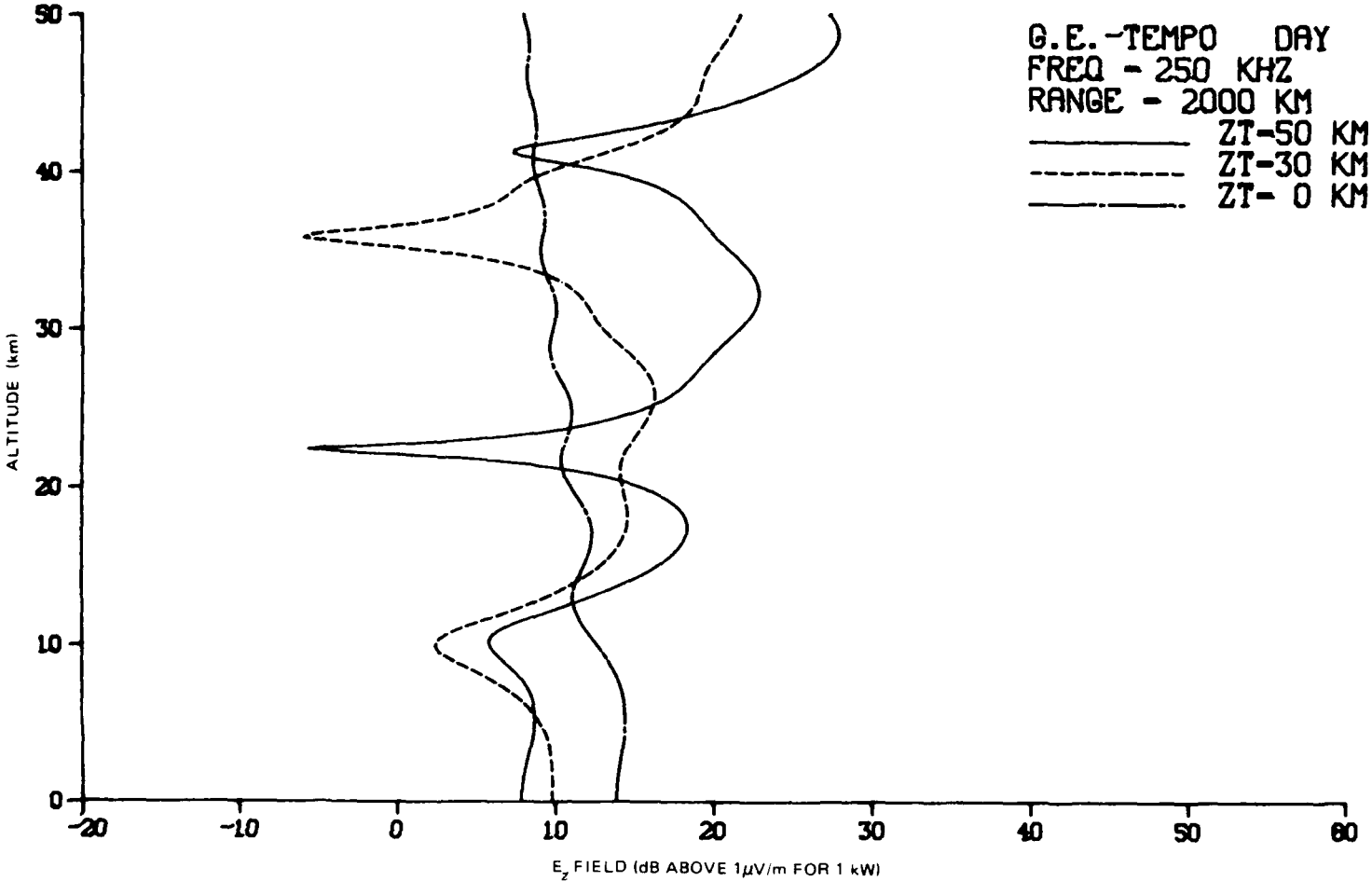

Figure 16. E_z as a function of height for GE-TEMPO day (250 kHz).

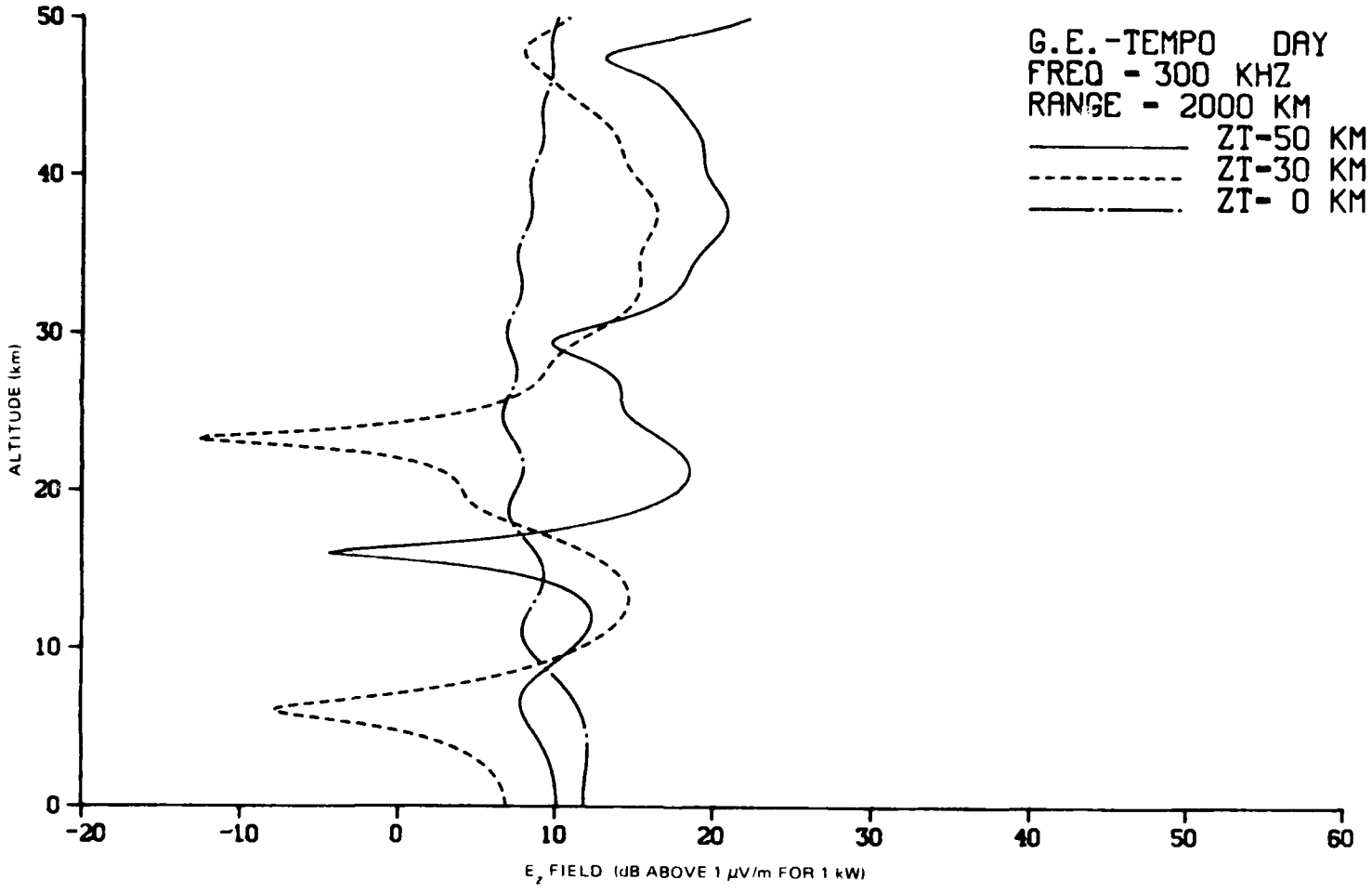

Figure 17. E_z as a function of height for GE-TEMPO day (300 kHz).

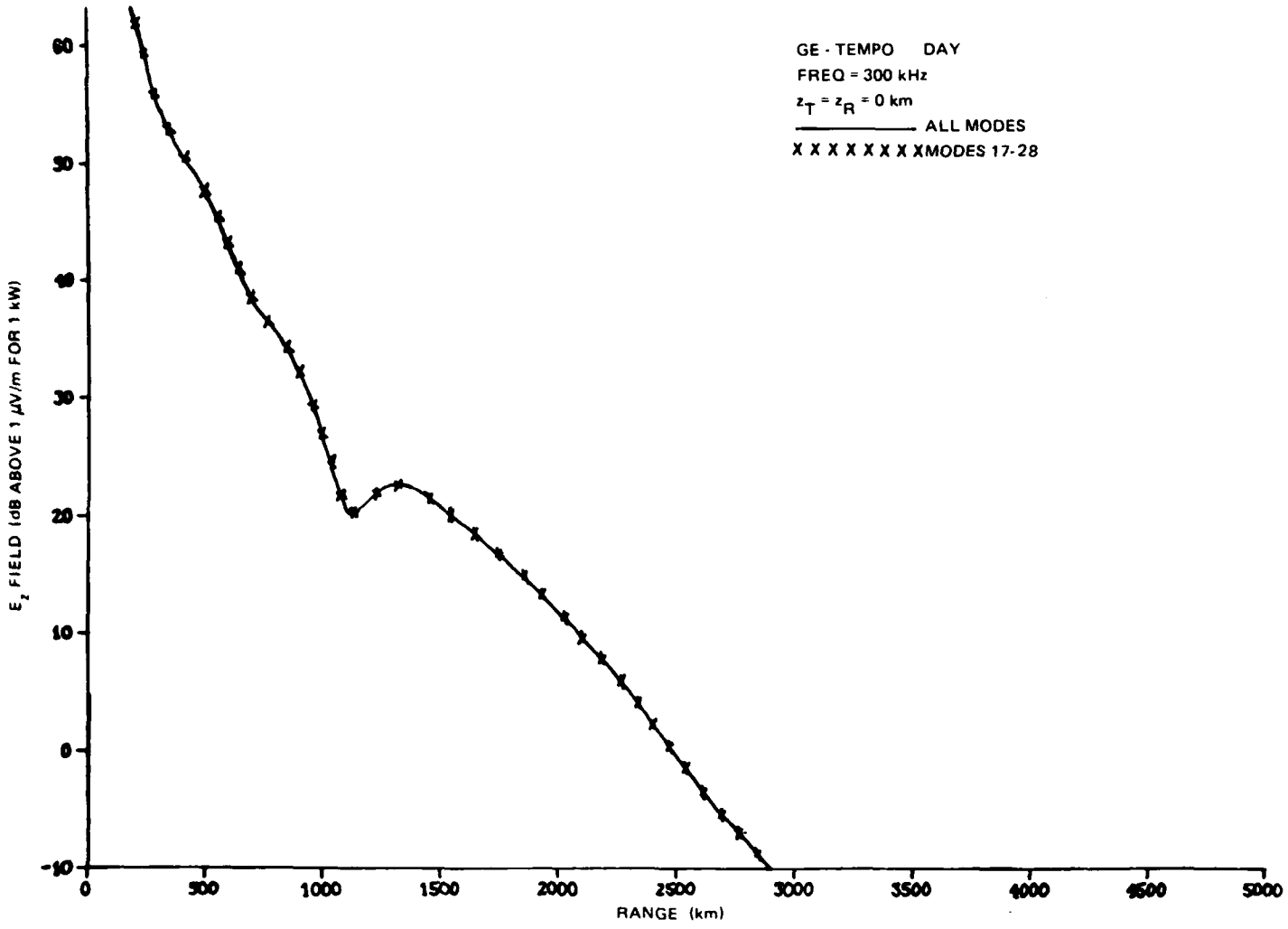

Figure 18. Range plot comparisons between full and truncated mode sums (300 kHz). Transmitter and receiver altitudes = 0 km.

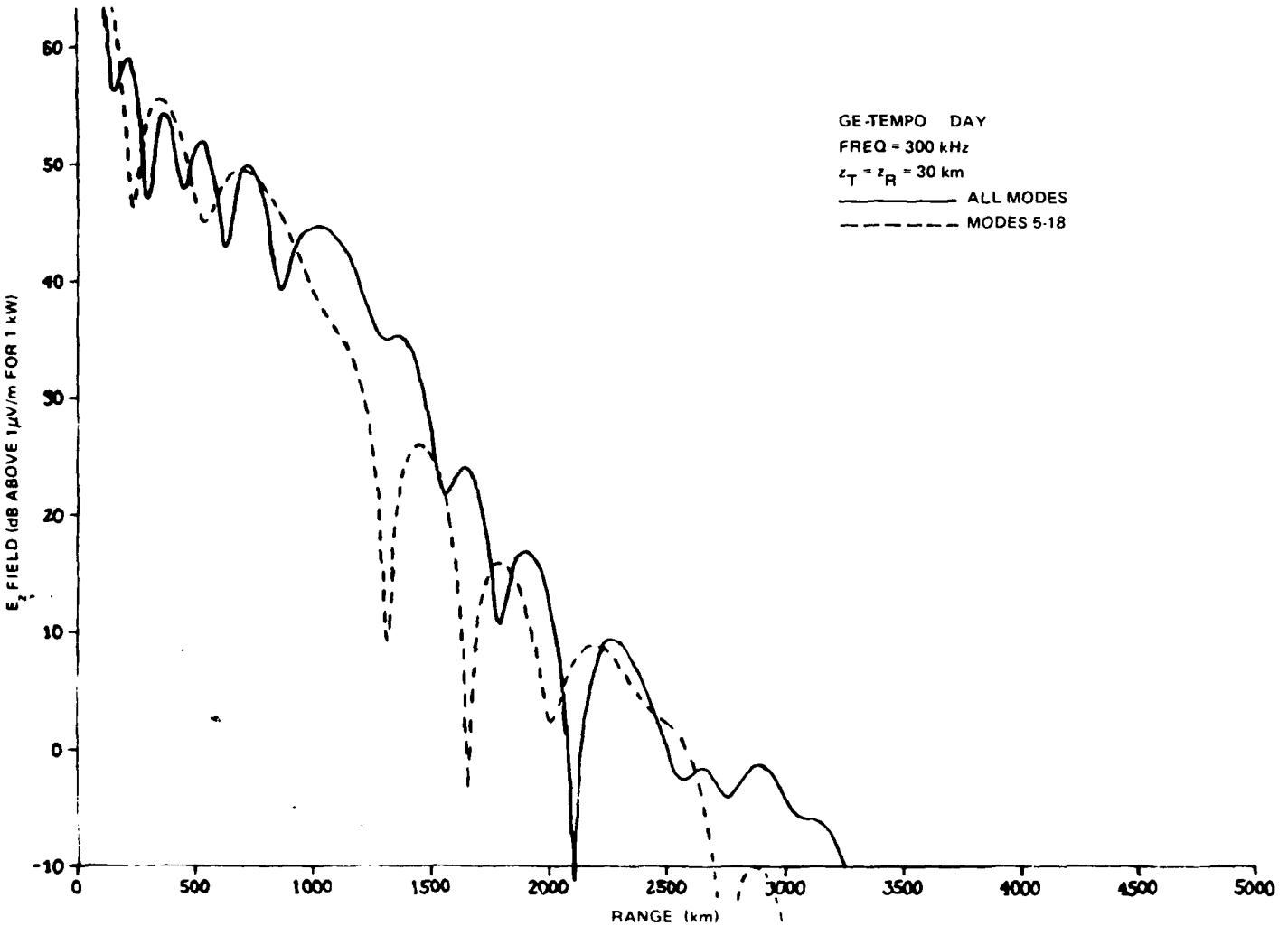

Figure 19. Range plot comparisons between full and truncated mode sums (300 kHz). Transmitter and receiver altitudes = 30 km.

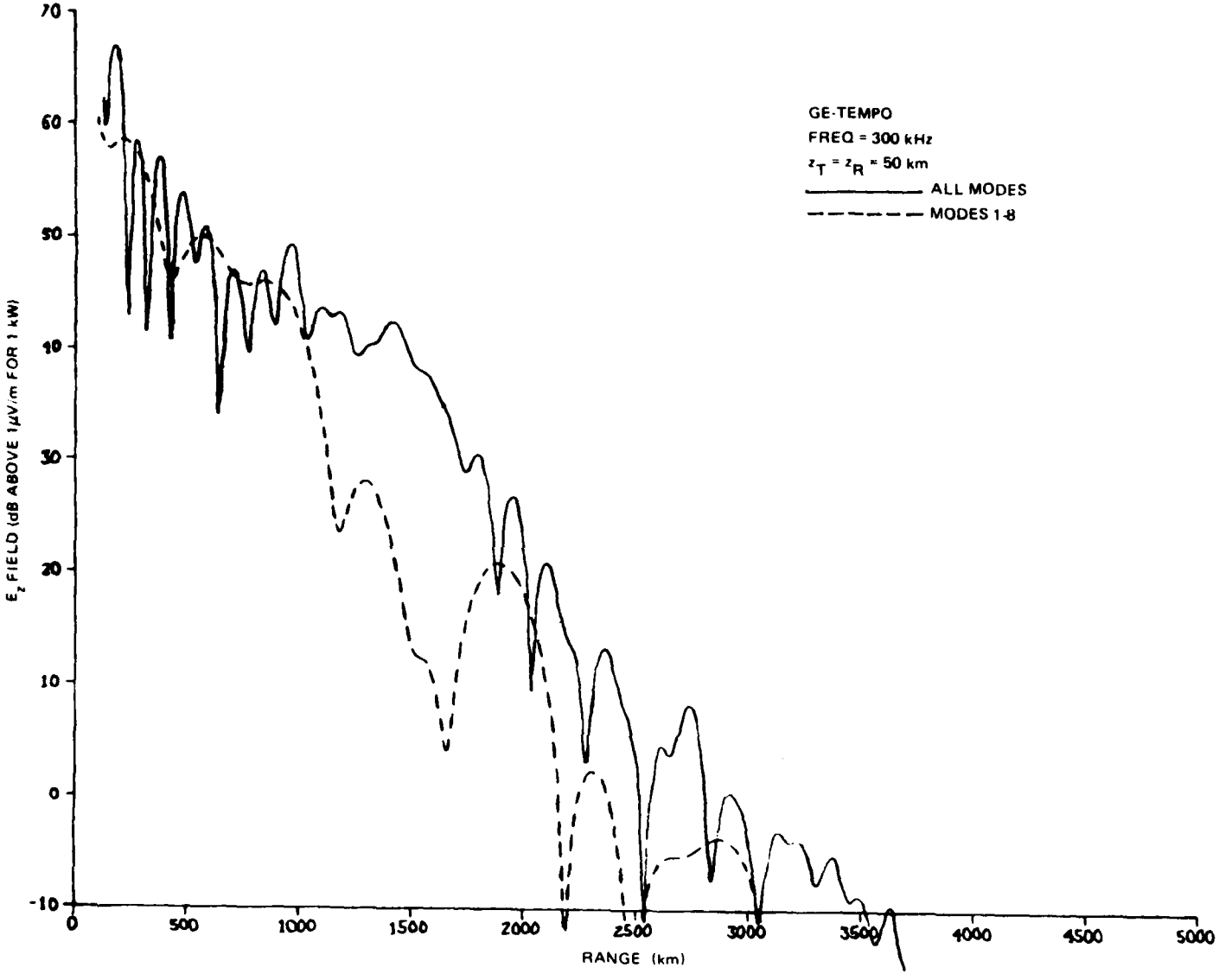

Figure 20. Range plot comparisons between full and truncated mode sums (300 kHz). Transmitter and receiver altitudes = 50 km.

DISTRIBUTION LIST

DEPARTMENT OF DEFENSE
ASSISTANT SECRETARY OF DEFENSE
CMD, CONT, COMM & INTELL
DEPARTMENT OF DEFENSE
WASHINGTON, DC 20301
M EPSTEIN
J BABCOCK

DIRECTOR
COMMAND CONTROL TECHNICAL CENTER
11440 ISAAC NEWTON SQUARE, N
RESTON, VA 22091
C-650

DIRECTOR
COMMAND CONTROL TECHNICAL CENTER
ROOM ME682, THE PENTAGON
WASHINGTON, DC 20301
C-312

DIRECTOR
DEFENSE ADVANCED RESEARCH PROJECT AGENCY
1400 WILSON BLVD
ARLINGTON, VA 22209
NUCLEAR MONITORING RSCH
STRATEGIC TECH OFFICE

DEFENSE COMMUNICATION ENGINEERING CENTER
1860 WIEHLE AVENUE
RESTON, VA 22090
CODE R220 (M HOROWITZ)
CODE R720 (JOHN WORTHINGTON)
CODE R410 (JAMES W McLEAN)
CODE R103

DIRECTOR
DEFENSE COMMUNICATIONS AGENCY
WASHINGTON, DC 20305
CODE 810 (RW ROSTRON)
CODE 480
CODE 101B (MAJ ROOD)

DEFENSE COMMUNICATIONS AGENCY
WWMCCS SYSTEM ENGINEERING ORG
WASHINGTON, DC 20305
RL CRAWFORD

DEFENSE TECHNICAL INFORMATION CENTER
CAMERON STATION
ALEXANDRIA, VA 22314
TC (12)

DIRECTOR
DEFENSE INTELLIGENCE AGENCY
WASHINGTON, DC 20301
DIAST-5
DIAAP (ALBERT L WISE)
DB-4C (EDWARD O'FARRELL)

DIRECTOR
DEFENSE NUCLEAR AGENCY
WASHINGTON, DC 20305
DDST
TISI ARCHIVES
TITL TECH LIBRARY (3)
RAAE (3)
STVL

COMMANDER
FIELD COMMAND
DEFENSE NUCLEAR AGENCY
KIRTLAND AFB, NM 87115
FCPR

DIRECTOR
INTERSERVICE NUCLEAR WEAPONS SCHOOL
KIRTLAND AFB, NM 87115
DOCUMENT CONTROL

DIRECTOR
JOINT STRAT TGT PLANNING STAFF JCS
OFFUTT AFB
OMAHA, NB 68113
JPST (CAPT DG GOETZ)

CHIEF
LIVERMORE DIVISION FLD COMMAND DNA
LAWRENCE LIVERMORE LABORATORY
PO BOX 808
LIVERMORE, CA 94550
FCPRL

DIRECTOR
NATIONAL SECURITY AGENCY
FT GEORGE G MEADE, MD 20755
W65
OLIVER H BARTLETT W32
TECHNICAL LIBRARY
JOHN SKILLMAN R52

OJCS/J 3
THE PENTAGON
WASHINGTON, DC 20301
OPERATIONS (WWMCCS EVAL OFF, MR TOMA)

OJCS/J 5
THE PENTAGON
WASHINGTON, DC 20301
PLANS & POLICY (NUCLEAR DIVISION)

UNDER SECRY OF DEFENSE FOR RESEARCH AND ENGINEERING
DEPARTMENT OF DEFENSE
WASHINGTON, DC 20301
S&SS (OS)

DEPARTMENT OF THE ARMY
COMMANDER/DIRECTOR
ATMOSPHERIC SCIENCES LABORATORY
US ARMY ELECTRONICS COMMAND
WHITE SANDS MISSILE RANGE, NM 88002
DELAS-AE-M (FE NILES)

COMMANDER
HARRY DIAMOND LABORATORIES
2800 POWDER MILL RD
ADELPHI, MD 20783
DELHD-NP (FRANCIES N WIMENITZ)
MILDRED H WEINER DRXDO-II

COMMANDER
US ARMY ELECTRONICS RESEARCH & DEVELOPMENT COMMAND
FORT MONMOUTH, NJ 07703
DRSEL-RD
(JE QUIGLEY)

COMMANDER
US ARMY FOREIGN SCIENCE & TECH CENTER
220 7TH STREET, NE
CHALOTTESVILLE, VA 22901
R JONES
PA CROWLEY

COMMANDER
US ARMY NUCLEAR AGENCY
7500 BACKLICK ROAD
BUILDING 2073
SPRINGFIELD, VA 22150
MONA-WE (J BERBERET)

CHIEF
US ARMY RESEARCH OFFICE
PO BOX 12211
TRIANGLE PARK, NC 27709
DRXRD-ZC

DEPARTMENT OF THE NAVY
CHIEF OF NAVAL OPERATIONS
NAVY DEPARTMENT
WASHINGTON, DC 20350
OP 941
OP-604C3
OP 943 (LCDR HUFF)
OP 981

CHIEF OF NAVAL RESEARCH
NAVY DEPARTMENT
ARLINGTON, VA 22217
CODE 402
CODE 420
CODE 421
CODE 461
CODE 464

COMMANDING OFFICER
NAVAL INTELLIGENCE SUPPORT CENTER
4301 SUITLAND RD BLDG 5
WASHINGTON, DC 20390

COMMANDER
NAVAL OCEAN SYSTEMS CENTER
SAN DIEGO, CA 92152
CODE 81 (HD SMITH)
CODE 532 (3)
CODE 532 (RICHARD A PAPPERT)

COMMANDING OFFICER
NAVAL RESEARCH LABORATORY
WASHINGTON, DC 20375
CODE 5410 (JOHN DAVIS)
CODE 7701 (JACK D BROWN)
CODE 5461 TRANS IONO PROP
CODE 5465 PROP APPLICATIONS
CODE 5460 ELECTROMAG PROP BR
CODE 2600 TECH LIBRARY (2)

OFFICER IN-CHARGE
WHITE OAK LABORATORY
NAVAL SURFACE WEAPONS CENTER
SILVER SPRING, MD 20910
CODE WA501 NAVY NUC PRGMS OFF
CODE WX21 TECH LIBRARY

COMMANDER
NAVAL TELECOMMUNCATIONS COMMAND
NAVTELCOM HEADQUARTERS
4401 MASSACHUSETTS AVE, NW
WASHINGTON, DC 20390
CODE 24C

COMMANDING OFFICER
NAVY UNDERWATER SOUND LABORATORY
FORT TRUMBULL
NEW LONDON, CT 06320
PETER BANNISTER
DA MILLER

DIRECTOR
STRATEGIC SYSTEMS PROJECT OFFICE
NAVY DEPARTMENT
WASHINGTON, DC 20376
NSP-2141

DEPARTMENT OF THE AIR FORCE
COMMANDER
ADC/DC
ENT AFB, CO 80912
DC (MR LONG)

COMMANDER
ADCOM/XPD
ENT AFB, CO 80912
XPQDQ
XP

AF GEOPHYSICS LABORATORY, AFSC
HASCOM AFB, MA 01731
CRU (S HOROWITZ)
PHP (JULES AARONS)
OPR (JAMES C ULWICK)
OPR (ALVA T STAIR)
SUOL (RESEARCH LIBRARY) (2)

AF WEAPONS LABORATORY, AFSC
KIRTLAND AFB, NM 87117
SUL (2)
SAS (JOHN M KAMM)
DYC (CAPT L WITTWER)

AFTAC
PATRICK AFB, FL 32925
TN
TD-3
TD-5
TF/MAJ WILEY

AIR FORCE AVIONICS LABORATORY, AFSC
WRIGHT-PATTERSON AFB, OH 45433
AAD

COMMANDER
FOREIGN TECHNOLOGY DIVISION, AFSC
WRIGHT-PATTERSON AFB, OH 45433
ETD BL BALLARD

HQ USAF/RD
WASHINGTON, DC 20330
RDQ

HEADQUARTERS
NORTH AMERICAN AIR DEFENSE COMMAND
1500 EAST BOULDER
COLORADO SPRINGS, CO 80912
CHIEF SCIENTIST

COMMANDER
ROME AIR DEVELOPMENT CENTER, AFSC
GRIFFISS AFB, NY 13440
EMTLD DOC LIBRARY

COMMANDER
ROME AIR DEVELOPMENT CENTER, AFSC
HANSCOM AFB, MA 01731
EEP JOHN RASMUSSEN

SAMSO/MN
NORTON AFB, CA 92409
MINUTEMAN (NMML LTC KENNEDY)

COMMANDER IN CHIEF
STRATEGIC AIR COMMAND
OFFUTT AFB, NB 68113
NRT
XPFS (MAJ BRIAN G STEPHAN)
DOK (CHIEF SCIENTIST)

US ENERGY RESEARCH AND DEV ADMIN
DEPARTMENT OF ENERGY
ALBUQUERQUE OPERATIONS OFFICE
PO BOX 5400
ALBUQUERQUE, NM 87115
DOC CON FOR D W SHERWOOD

DIVISION OF MILITARY APPLICATION
DEPARTMENT OF ENERGY
WASHINGTON, DC 20545
DOC CON FOR DONALD I GALE

LAWRENCE LIVERMORE LABORATORY
PO BOX 808
LIVERMORE, CA 94550
GLENN C WERTH L-216
TECH INFO DEPT L-3

LOS ALAMOS SCIENTIFIC LABORATORY
PO BOX 1663
LOS ALAMOS, NM 87545
DOC CON FOR T F TASCHEK
DOC CON FOR D R WESTERVELT
DOC CON FOR P W KEATON
DOC CON FOR J H COON

SANDIA LABORATORIES
LIVERMORE LABORATORY
PO BOX 969
LIVERMORE, CA 94550
DOC CON FOR B E MURPHEY
DOC CON FOR T B COOK ORG 8000

SANDIA LABORATORIES
PO BOX 5800
ALBUQUERQUE, NM 87115
DOC CON FOR SPACE PROJ DIV
DOC CON FOR A D THORNBROUGH, ORG 1245
DOC CON FOR W C MYRA
DOC CON FOR 3141 SANDIA RPT COLL

OTHER GOVERNMENT
DEPARTMENT OF COMMERCE
NATIONAL BUREAU OF STANDARDS
WASHINGTON, DC 20234
RAYMOND T MOORE

DEPARTMENT OF COMMERCE
OFFICE OF TELECOMMUNICATIONS
INSTITUTE FOR TELCOM SCIENCE
BOULDER, CO 80302
WILLIAM F UTLAUT
L A BERRY
A GLENN JEAN
D D CROMBIE
J R WAIT

DEPARTMENT OF TRANSPORTATION
OFFICE OF THE SECRETARY
TAD-44.1, ROOM 10402-B
400 7TH STREET, SW
WASHINGTON, DC 20590
R L LEWIS
R H DOHERTY

DEPARTMENT OF DEFENSE CONTRACTORS
AEROSPACE CORPORATION
PO BOX 92957
LOS ANGELES, CA 90009
IRVING M GARFUNKEL

ANALYTICAL SYSTEMS ENGINEERING CORP
5 OLD CONCORD RD
BURLINGTON, MA 01803
RADIO SCIENCES

THE BOEING COMPANY
PO BOX 3707
SEATTLE, WA 98124
GLENN A HALL
J F KENNEY

UNIVERSITY OF CALIFORNIA
AT SAN DIEGO
MARINE PHYSICAL LAB OF THE
SCRIPPS INSTITUTE OF OCEANOGRAPHY
SAN DIEGO, CA 92132
HENRY G BOOKER

COMPUTER SCIENCES CORPORATION
PO BOX 530
6565 ARLINGTON BLVD
FALLS CHUCH, VA 22046
D BLUMBERG

UNIVERSITY OF DENVER
COLORADO SEMINARY
DENVER RESEARCH INSTITUTE
PO BOX 10127
DENVER, CO 80210
DONALD DUBBERT
HERBERT REND

ESL, INC
495 JAVA DRIVE
SUNNYVALE, CA 94086
JAMES MARSHALL

GENERAL ELECTRIC COMPANY
SPACE DIVISION
VALLEY FORGE SPACE CENTER
GODDARD BLVD KING OF PRUSSIA
PO BOX 8555
PHILADELPHIA, PA 19101
SPACE SCIENCE LAB (MH BORTNER)

GENERAL ELECTRIC COMPANY
TEMPO-CENTER FOR ADVANCED STUDIES
816 STATE STREET
PO DRAWER QQ
SANTA BARBARA, CA 93102
B GAMBILL
DASIAC (2)
DON CHANDLER
WARREN S KNAPP

GEOPHYSICAL INSTITUTE
UNIVERSITY OF ALASKA
FAIRBANKS, AK 99701
T N DAVIS
NEAL BROWN
TECHNICAL LABORATORY

GTE SYLVANIA, INC
ELECTRONICS SYSTEMS GRP
EASTERN DIVISION
77 A STREET
NEEDHAM, MA 02194
MARSHAL CROSS

IIT RESEARCH INSTITUTE
10 WEST 35TH STREET
CHICAGO, IL 60616
TECHNICAL LIBRARY

UNIVERSITY OF ILLINOIS
DEPARTMENT OF ELECTRICAL ENGINEERING
URBANA, IL 61803
AERONOMY LABORATORY (2)

JOHNS HOPKINS UNIVERSITY
APPLIED PHYSICS LABORATORY
JOHNS HOPKINS ROAD
LAUREL, MD 20810
J NEWLAND
PT KOMISKE

LOCKHEED MISSILES & SPACE CO, INC
3251 HANOVER STREET
PALO ALTO, CA 94304
E E GAINES
W L IMHOF D/52-12
J B REAGAN 0652-12
R G JOHNSON D/52-12

LOWELL RESEARCH FOUNDATION
450 AIKEN STREET
LOWELL, MA 01854
DR BIBL

MASSACHUSETTS INSTITUTE OF TECHNOLOGY
LINCOLN LABORATORY
PO BOX 73
LEXINGTON, MA 02173
DAVE WHITE
J H PANNELL L 246
D M TOWLE

MISSION RESEARCH CORPORATION
735 STATE STREET
SANTA BARBARA, CA 93101
R HENDRICK
F FAJEN
M SCHEIBE
J GILBERT
C L LONGMIRE

MITRE CORPORATION
PO BOX 208
BEDFORD, MA 01730
G HARDING

PACIFIC-SIERRA RESEARCH CORP
1456 CLOVERFIELD BLVD
SANTA MONICA, CA 90404
E C FIELD, JR

PENNSYLVANIA STATE UNIVERSITY
IONOSPHERIC RESEARCH LABORATORY
318 ELECTRICAL ENGINEERING EAST
UNIVERSITY PARK, PA 16802
IONOSPHERIC RSCH LAB (2)

R&D ASSOCIATES
PO BOX 9695
MARINA DEL REY, CA 90291
FORREST GILMORE
WILLIAM J KARZAS
PHYLLIS GREIFINGER
CARL GREIFINGER
A ORY
BRYAN GABBARD
R P TURCO
SAUL ALTSCHULER

RAND CORPORATION
1700 MAIN STREET
SANTA MONICA, CA 90406
TECHNICAL LIBRARY (2)
CULLEN CRAIN

SRI INTERNATIONAL
333 RAVENSWOOD AVENUE
MENLO PARK, CA 94025
DONALD NEILSON
GEORGE CARPENTER
W G CHESNUT
J R PETERSON
GARY PRICE

STANFORD UNIVERSITY
RADIO SCIENCE LABORATORY
STANFORD, CA 94305
R A HELLIWELL
FRASER SMITH
J KATSUFRAKIS

TRW DEFENSE & SPACE SYS GROUP
ONE SPACE PARK
REDONDO BEACH, CA 90278
DIANA DEE

CALIFORNIA INSTITUTE OF TECHNOLOGY
JET PROPULSION LABORATORY
4800 OAK GROVE DRIVE
PASADENA, CA 91103
ERNEST K SMITH
(MAIL CODE 144-B13)

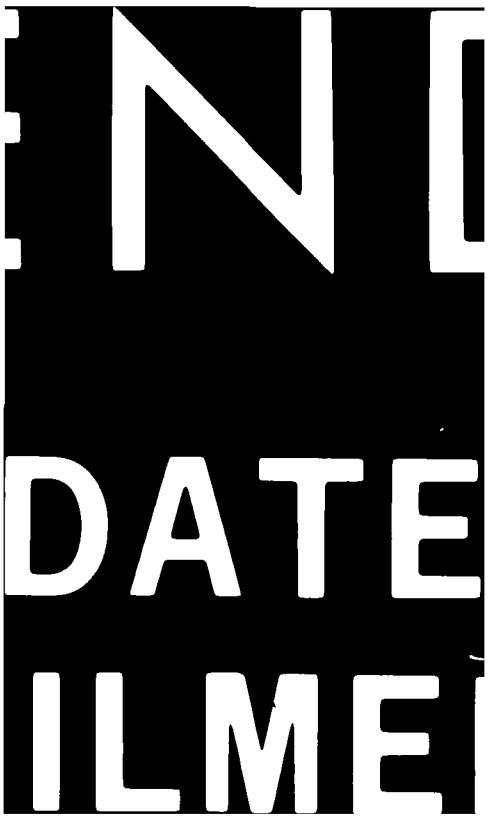
N
DATE
ILME